

Unique $\{H(SiR_3)_2\}$, (H_2SiR_3) , $H(HSiR_3)$, and $(H_2)SiR_3$ Ligand Sets Supported by the $\{Fe(Cp)(L)\}$ Platform ($L = CO, PR_3$)

Sergei F. Vyboishchikov*^[a] and Georgii I. Nikonov*^[b]

Dedicated to Professor Dr. Gernot Frenking on the occasion of his 60th birthday

Abstract: This work deals with the type and incidence of nonclassical Si–H and H–H interactions in a family of silylhydride complexes $[Fe(Cp)(OC)(SiMe_nCl_{3-n})H(X)]$ ($X = SiMe_nCl_{3-n}, H, Me, n = 0–3$) and $[Fe(Cp)(Me_3P)(SiMe_nCl_{3-n})_2H]$ ($n = 0–3$). DFT calculations complemented by atom-in-molecule analysis and calculations of NMR hydrogen–silicon coupling constants revealed a surprising diversity of nonclassical Si–H and H–H interligand interactions. The compounds $[Fe(Cp)(L)(SiMe_nCl_{3-n})_2H]$ ($L = CO, PMe_3; n = 0–3$) exhibit an unusual distortion from the ideal piano-stool geometry in that the silyl ligands are strongly shifted toward the hydride and

there is a strong trend towards flattening of the $\{FeSi_2H\}$ fragment. Such a distortion leads to short Si–H contacts (range 2.030–2.075 Å) and large Mayer bond orders. A novel feature of these extended Si–H interactions is that they are rather insensitive towards the substitution at the silicon atom and the orientation of the silyl ligand relatively the Fe–H bond. NMR spectroscopy and bonding features of the related complexes $[Fe(Cp)(OC)(SiMe_nCl_{3-n})H(Me)]$ ($n = 0–3$) allow for their ration-

Keywords: hydrides • hypervalent compounds • sigma complexes • silicon

alization as usual η^2 -Si–H silane σ -complexes. The series of “dihydride” complexes $[Fe(Cp)(OC)(SiMe_nCl_{3-n})H_2]$ ($n = 0–3$) is different from the previous two families in that the type of interligand interactions strongly depends on the substitution on silicon. They can be classified either as usual dihydrogen complexes, for example, $[Fe(Cp)(OC)(SiMe_2Cl)(\eta^2-H_2)]$, or as compounds with nonclassical H–Si interactions, for example, $[Fe(Cp)(OC)(H)_2(SiMe_3)]$ (**16**). These nonclassical interligand interactions are characterized by increased negative $J(H,Si)$ (e.g. –27.5 Hz) and increased $J(H,H)$ (e.g. 67.7 Hz).

Introduction

Transition-metal-mediated transformations of small molecules are of central importance to catalysis.^[1] Among different X–Y bond rupture/formation reactions the activation of H–H,^[2] H–C,^[3] and H–Si^[4,5] bonds have received most theo-

retical treatment due to their relevance to a range of important catalytic reactions, such as hydrogenation, alkane functionalization, hydrosilation, and so forth,^[1] and due to the simplicity of hydride as a 1s electron ligand.^[2] While earlier work has been focused primarily on theoretical rationalization of metal–ligand bonding in the starting and final compounds, current research shifts more towards the understanding of the reaction mechanisms, which to a great extent deals with elucidating the nature of interligand interactions in reactive intermediates and transition states.

The discovery and investigation of σ -complexes and agostic complexes provided convincing proof for the validity of this concept by revealing key factors controlling the course of oxidative addition reactions.^[6,7] Among many types of nonclassical Y–X bonds, those between hydrogen and silicon exhibit particularly large diversity due to the propensity of silicon to be hypervalent and expand its coordination sphere^[4e-g,8,9] At least in some cases, compounds featuring hypervalent silicon environments of the type η^4 - H_3SiR_3 and η^3 - H_2SiR_3 can be rationalized as those with distorted hypervalent silyl ligands $(H_3SiR_3)^{2-}$ and $(H_2SiR_3)^{-}$.^[8]

[a] Dr. S. F. Vyboishchikov
Institut de Química Computacional
Campus de Montilivi, Universitat de Girona
17071 Girona, Catalonia (Spain)
Fax: (+34) 97241-8356
E-mail: vybo@stark.udg.es

[b] Dr. G. I. Nikonov
Chemistry Department, Brock University
500 Glenridge Ave., St. Catharines, ON, L2S 3 A1 (Canada)
Fax: (+1) 905-682-9020
E-mail: gnikonov@brocku.ca

Supporting information for this article is available on the WWW under <http://www.chemeurj.org/> or from the author. It contains the complete reference [11] and Tables SII–4 give the relative stabilities of rotamers a–c.

Abstract in German: In dieser Arbeit handelt es sich um den Charakter nichtklassischer Si–H- und H–H-Wechselwirkungen in einer Klasse der Silylhydridkomplexe $[\text{Fe}(\text{Cp})(\text{OC})(\text{SiMe}_n\text{Cl}_{3-n})\text{H}(\text{X})]$ ($\text{X} = \text{SiMe}_n\text{Cl}_{3-n}$, H , Me , $n=0-3$) und $[\text{Fe}(\text{Cp})(\text{Me}_3\text{P})(\text{SiMe}_n\text{Cl}_{3-n})_2\text{H}]$ ($n=0-3$). Die DFT-Berechnungen, durch die Bader-Analyse und die Berechnungen der NMR-Silizium-Wasserstoff-Kopplungskonstanten ergänzt, decken eine überraschende Vielfältigkeit der nichtklassischen Si–H- und H–H-Interligandwechselwirkungen auf. Die Verbindungen $[\text{Fe}(\text{Cp})(\text{L})(\text{SiMe}_n\text{Cl}_{3-n})_2\text{H}]$ ($\text{L} = \text{CO}$, PMe_3 ; $n=0-3$) weisen eine ungewöhnliche Verzerrung von der idealen Klavierstuhlgeometrie auf. Die Silylliganden werden stark in Richtung zum Hydrid hin verschoben und es gibt einen deutlichen Trend zur Planarisierung des FeSi_2H -Fragmentes. Eine solche Verzerrung führt zu kurzen Si–H-Kontakten (2.030–2.075 Å) und hohen Mayer-Bindungsordnungen. Eine neue Besonderheit dieser verlängerten Si–H-Wechselwirkungen ist, dass sie ziemlich unempfindlich in bezug auf die Substituenten am Siliziumatom und die Orientierung des Silylliganden bezüglich der Fe–H-Bindung sind. Die NMR-Eigenschaften und das Bindungsbild der verwandten Komplexe $[\text{Fe}(\text{Cp})(\text{OC})(\text{SiMe}_n\text{Cl}_{3-n})\text{H}(\text{Me})]$ ($n=0-3$) lassen deren Interpretation als herkömmliche η^2 -Si–H-Silan- σ -Komplexe zu. Die Reihe von "Dihydrid"-Komplexen $[\text{Fe}(\text{Cp})(\text{OC})(\text{SiMe}_n\text{Cl}_{3-n})\text{H}_2]$ ($n=0-3$) unterscheidet sich von den beiden vorhergehenden Klassen dadurch, dass der Typ der Interligandwechselwirkungen stark von Substituenten am Silizium abhängt. Sie können entweder als herkömmliche Diwasserstoffkomplexe, z.B., $[\text{Fe}(\text{Cp})(\text{OC})(\text{SiMe}_2\text{Cl})(\eta^2\text{-H}_2)]$, oder als Verbindungen mit nichtklassischen H–Si-Wechselwirkungen, z.B., $[\text{Fe}(\text{Cp})(\text{OC})(\text{H})_2(\text{SiMe}_3)]$ (16) eingestuft werden. Diese nichtklassischen Interligandwechselwirkungen zeichnen sich durch ein erhöhtes negatives $J(\text{H},\text{Si})$ (z.B. –27,5 Hz) und erhöhtes $J(\text{H},\text{H})$ (z.B. 67,7 Hz) aus.

Настоящая работа посвящена изучению неклассических взаимодействий Si–H и H–H в семействе силилгидридных комплексов $[\text{Fe}(\text{Cp})(\text{OC})(\text{SiMe}_n\text{Cl}_{3-n})\text{H}(\text{X})]$ ($\text{X} = \text{SiMe}_n\text{Cl}_{3-n}$, H , Me , $n=0-3$) и $[\text{Fe}(\text{Cp})(\text{Me}_3\text{P})(\text{SiMe}_n\text{Cl}_{3-n})_2\text{H}]$ ($n=0-3$). Расчёты с помощью теории функционала плотности, а также топологический анализ электронной плотности и расчёт констант спин-спинового взаимодействия Si–H выявили неожиданное разнообразие типов неклассических межлигандных взаимодействий Si–H и H–H в этих комплексах. Найдено, что в соединениях $[\text{Fe}(\text{Cp})(\text{L})(\text{SiMe}_n\text{Cl}_{3-n})_2\text{H}]$ ($\text{L} = \text{CO}$, PMe_3 ; $n=0-3$) проявляется необычное искажение от идеальной геометрии фортепианной табуретки, которые проявляются в сильном смещении силильных лигандов в сторону гидрида. Кроме того, имеется явная тенденция к уплощению фрагмента FeSi_2H . Такое искажение приводит к коротким контактам Si–H (в диапазоне 2.030–2.075 Å) и соответствующим высоким порядкам связи по Майеру. Новая особенность таких удлинённых взаимодействий Si–H состоит в том, что они почти не зависят от природы заместителей при атоме кремния и ориентации силильного лиганда относительно связи Fe–H. Напротив, особенности вычисленных ЯМР параметров и параметров связей Si–H в родственных комплексах $[\text{Fe}(\text{Cp})(\text{OC})(\text{SiMe}_n\text{Cl}_{3-n})\text{H}(\text{Me})]$ ($n=0-3$) позволяют описывать эти структуры как обычные η^2 -Si–H σ -комплексы силанов. Серия «дигидридных» комплексов $[\text{Fe}(\text{Cp})(\text{OC})(\text{SiMe}_n\text{Cl}_{3-n})\text{H}_2]$ ($n=0-3$) отличается от двух предыдущих семейств тем, что характер межлигандных взаимодействий сильно зависит от заместителей при атоме кремния. Их можно отнести либо к обычным комплексам молекулярного водорода, например, $[\text{Fe}(\text{Cp})(\text{OC})(\text{SiMe}_2\text{Cl})(\eta^2\text{-H}_2)]$, или к соединениям с неклассическими взаимодействиями H–Si, например, $[\text{Fe}(\text{Cp})(\text{OC})(\text{H})_2(\text{SiMe}_3)]$ (16). Эти неклассические межлигандные взаимодействия характеризуются повышенным отрицательным $J(\text{H}-\text{Si})$ (например, –27,5 Гц) и повышенным $J(\text{H}-\text{H})$ (например, 67,7 Гц).

The η^3 -coordination of a silane ligand has been experimentally observed in the binuclear silane-bridged complex $[\{\text{Ru}(\text{C}_3\text{P}_2)_2\text{H}_2\}(\mu\text{-}\eta^3\text{-}\eta^3\text{-SiH}_4)]$.^[9d] Also, the $\eta^3\text{-H}_2\text{SiH}_3$ ligand was calculated to lie only 0.5 kcal mol^{–1} above the $(\eta^2\text{-HSiH}_3)\text{H}$ alternative in the model compound $[\text{Ru}(\text{Tp})(\text{H}_3\text{P})(\text{H}_2\text{SiH}_3)]$ ($\text{Tp} = \text{tris}(\text{pyrazolyl})\text{borate}$).^[4q] Its prototypical complexes $[\text{Ru}(\text{Tp})(\text{Ph}_3\text{P})(\text{H}_2\text{SiR}_3)]$ are highly fluxional, which was interpreted as being due to an equilibrium between two η^2 -silane forms: $[\text{Ru}(\text{L})_n(\text{H}^a)(\eta\text{-H}^b\text{-SiR}_3)]$ and $[\text{Ru}(\text{L})_n(\eta\text{-H}^a\text{-SiR}_3)\text{H}^b]$. Surprisingly enough, an NMR study of $[\text{Ru}(\text{Tp})(\text{Ph}_3\text{P})(\text{H}_2\text{SiR}_3)]$ revealed the largest $J(\text{H},\text{Si})$ spin–spin coupling constant of 52.8 Hz for the most electron-withdrawing R groups at silicon (in this case for $\text{R}_3 = (\text{OEt})_3$).^[4q] This observation contradicts the common trend that in silane σ -complexes electron-withdrawing substituents lead to weaker H–Si interaction and, presumably, to smaller $J(\text{H},\text{Si})$ coupling constants.^[10] This discrepancy suggests that a ligand motif more complex than the usual $(\eta^2\text{-HSiR}_3)\text{H}$ or $(\eta^2\text{-HSiR}_3)\text{SiR}_3$ can occur in these and related systems.^[8]

The main factors controlling the formation of complexes of such unconventional ligands $(\eta^3\text{-H}_2\text{X})^-$ versus classical complexes $[\text{M}(\text{L})_n\text{H}_2\text{X}]$ can be understood from a MO interaction diagram describing the interaction of an $(\text{HXH})^-$ ion with a metal fragment $\{\text{M}(\text{L})_n\}$ (Figure 1). There are two ligand-to-metal donation components (of the a' and a'' symmetry, if a local C_s symmetry is assumed), and a metal-to-ligand back-donation component of the symmetry a' . The efficiency of the latter will determine the extent of H–X bond splitting. Therefore, the main factors controlling the formation of complexes $[\text{M}(\text{L})_n(\eta^3\text{-H}_2\text{X})]$ are apparently the same as for the more common σ -complexes $[\text{M}(\text{L})_n(\eta^2\text{-HX})]$. These factors are: 1) the presence of a metal from the first transition series (such metals feature rather corelike 3d orbitals, not effective in back-donation to ligand-based antibonding orbitals of π symmetry), 2) the presence of π -accepting or σ -electron-withdrawing ligands, 3) the presence of a positive charge in the complex, and 4) high oxidation state of the metal.^[6b] Having these prerequisites in mind and wishing to establish the conditions for the existence of ligands of the type YHX , we set up to investigate a series of silyl-hydride complexes $[\text{Fe}(\text{Cp})(\text{OC})(\text{SiMe}_n\text{Cl}_{3-n})\text{H}(\text{X})]$ ($\text{X} = \text{H}$, Me , $\text{SiMe}_n\text{Cl}_{3-n}$; $n=0-3$) and $[[\text{Fe}(\text{Cp})(\text{Me}_3\text{P})(\text{SiMe}_n\text{Cl}_{3-n})_2\text{H}(\text{X})]$ ($n=0-3$), using computational chemistry methods. We reckoned that the combination of a small 3d metal, such as iron, in a relatively high oxidation state, with a π -accepting ligand could cause the formation of nonclassical interligand interactions in the coordination sphere of the metal. By varying the nature of ligands L and the substituents at silicon atom, we intended to determine the conditions for the formation of a classical ligand set $(\text{X})(\text{H})(\text{SiR}_3)$ versus nonclassical sets $(\text{SiR}_3)(\eta^2\text{-HX})$ and, possibly, (XHSiR_3) .

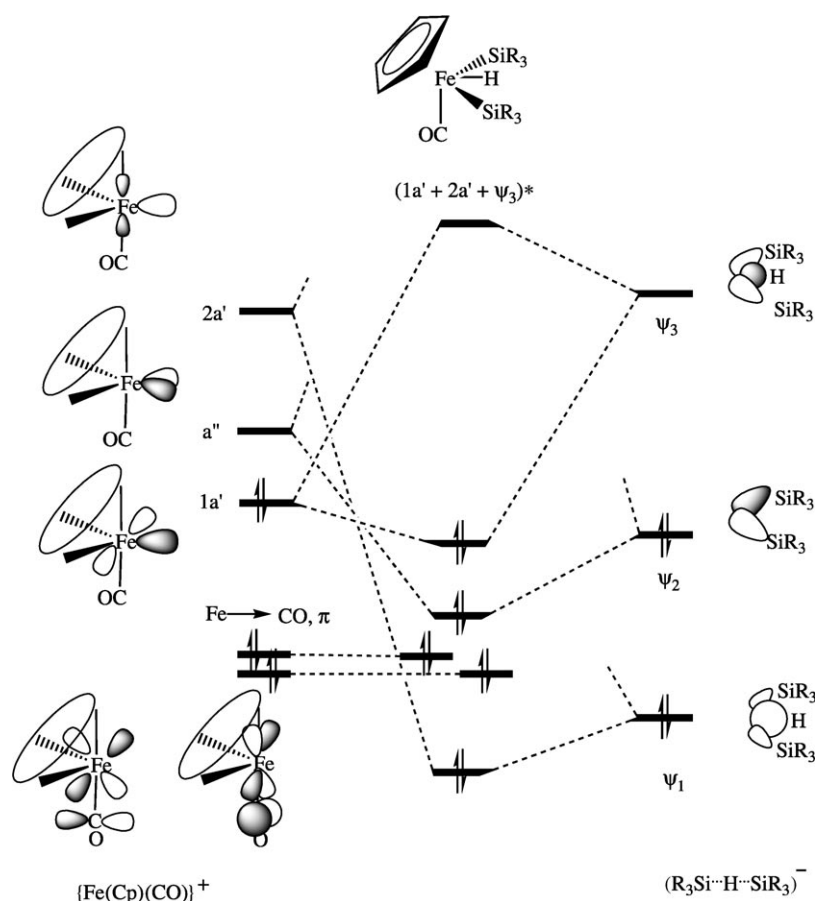


Figure 1. Molecular orbital interaction diagram for $[\text{Fe}(\text{Cp})(\text{OC})(\text{SiR}_3)_2\text{H}]$. The MOs of the fragment $\{\text{Fe}(\text{Cp})(\text{CO})\}^+$ can be considered as derived from a pseudo-octahedral structure $[\text{Fe}(\text{Cp})(\text{CO})(\text{L})_2]^+$ upon the removal of two *cis* ligands L. The complex $[\text{Fe}(\text{Cp})(\text{CO})(\text{L})_2]^+$ is octahedral, taking into account the isolobal relationship between the Cp^- ligand and a set of three *fac*-CO ligands, so that the Cp^- ligand occupies a facet of an octahedron.

Computational Methods

All geometry optimizations were carried out by using the density-functional theory with the Gaussian 03 program package^[11] applying the Perdew–Burke–Ernzerhof exchange and correlation functionals (PBE–PBE).^[12] For iron, we used the all-electron triple- ζ valence basis set augmented by one polarization *p* function (contraction Scheme {842111/6311/411}) of Ahlrichs and co-workers.^[13] On other atoms, the standard 6–311G** basis was employed. In the text we will refer to this basis set combination as “normal basis”. Full geometry optimizations without symmetry constraints were performed for all the molecular structures under study. The Mayer bond orders^[14] (in atomic orbital basis) and Wiberg bond orders^[15] (in natural atomic orbital basis) were also evaluated, by using the Gaussian 03 program. In some cases, we additionally evaluated three-center bond indices^[16] by using a program written by the authors. The spin–spin coupling constants $J(^1\text{H},^{29}\text{Si})$ for the complexes under study were calculated within the gauge-including atomic orbitals (GIAO) approach^[17] by using the Gaussian 03 program. Taking into account the high sensitivity of magnetic values to the basis set and to the density functional, more extended basis sets were used for the NMR calculations. These correspond to the completely decontracted “IGLO-III” basis set of Kutzelnigg and co-workers.^[18] To provide better flexibility in the core region, which is important for coupling constants,^[19] it was augmented by one steep *s*-function at silicon and hydrogen. We refer to the resulting basis set as “de-IGLO-III-ext”. As hybrid functionals were shown to perform more reliably for spin–spin coupling constants,^[19] the NMR param-

eters were calculated by using the B3LYP functional^[20] with the “de-IGLO-III-ext” basis set at the silyl and hydride ligands. On other atoms, the original basis used for optimization was retained. Test calculations of $J(^1\text{H},^{29}\text{Si})$ with the more sophisticated Becke-97 hybrid exchange correlation functional^[21] yielded values almost identical to the B3LYP ones.

Results and Discussion

Bis(silyl)–carbonyl complexes $[\text{Fe}(\text{Cp})(\text{OC})(\text{SiR}_3)_2\text{H}]$ —experimental data:

The compound $[\text{Fe}(\text{Cp})(\text{OC})(\text{SiCl}_3)_2\text{H}]$ (**1**) was among the first ones for which a hydride–silicon coupling constant $J(\text{H},\text{Si})$ was determined experimentally.^[22] The value of 20 Hz was measured from silicon satellites of the hydride signal in the ^1H NMR spectrum of **1**; similar $J(\text{H},\text{Si})$ were observed for the related compounds $[\text{Fe}(\text{Cp})(\text{OC})(\text{SiPh}_3)(\text{H})(\text{SnPh}_3)]$ ($J(\text{H},\text{Si}) = 23 \text{ Hz}$)^[23a] and $[\text{Fe}(\text{Cp})(\text{OC})(\text{SiHMe}_2)_2(\text{H})]$ ($J(\text{H},\text{Si}) = 12.9 \text{ Hz}$).^[23b] NMR coupling constants of such a magnitude have been long regarded as indicative of the absence of any significant interaction between

the hydride and silyl ligands.^[10] The X-ray structure of **1** was inconclusive in this regard as the hydride ligand was not determined.^[24] Two other X-ray structures of related silyl complexes, $[\text{Fe}(\text{Cp})(\text{CO})(\text{H})(\text{SiF}_2\text{CH}_3)_2]$ ^[25] and $[\text{Fe}(\text{Cp})(\text{CO})(\text{H})\{\text{SiPh}(\text{CH}_3)_2\}_2]$ ^[26] are also available. The hydride ligand was found for the former at the Si–H distance of 2.06(7) Å. In spite of the well-known uncertainty in finding hydrides in heavy element environments, this value provides a very good estimate for the silicon–hydride contact, because the variation of the Fe–H distance in the range 1.4–1.6 Å gives only a minor variation of the Si–H distance (range of 2.04–2.09 Å). The Si–H contact is not really dependent on the value of the Ct–Fe–H bond angle (where Ct is the centroid of the Cp ring) either, since changing this angle from 117.5° to 127.5° corresponds to varying the Si–H distance in the narrow range of 2.02–2.11 Å. Therefore, the observed Si–H distance is mainly the result of a small Si–Fe–Si bond angle (113.9(1)°), which suggests that similar Si–H contacts should exist in the other two compounds too. The molecular parameters of all three iron complexes are consistent with a symmetrical or nearly symmetrical structure. Taking into account the presence of relatively short H–Si distances, this

may suggest the presence of two equivalent weak Si–H interactions, for example, in the form of a distorted $(R_3Si-H-SiR_3)^-$ ligand.

DFT calculation of bis(silyl)–carbonyl complexes $[Fe(Cp)(OC)(SiMe_nCl_{3-n})_2H]$ —bonding model: In this work we report DFT calculations of a series of bis(silyl)hydride complexes $[Fe(Cp)(OC)(SiMe_nCl_{3-n})_2H]$ (**1–4**) bearing different

substituents at the silyl centers ($n=0$ (**1**), 1 (**2**), 2 (**3**), 3 (**4**), Figure 2). The selected computed molecular parameters are given in Table 1. For compounds with a substituent at silicon different from the other two substituents, there are three non-equivalent orientations of the silyl group depending on whether this unique substituent is oriented *trans* to the hydride (*trans*), towards the Cp ring (up), or opposite to the ring (down). In total, this gives rise to $3 \times 3 = 9$ different ro-

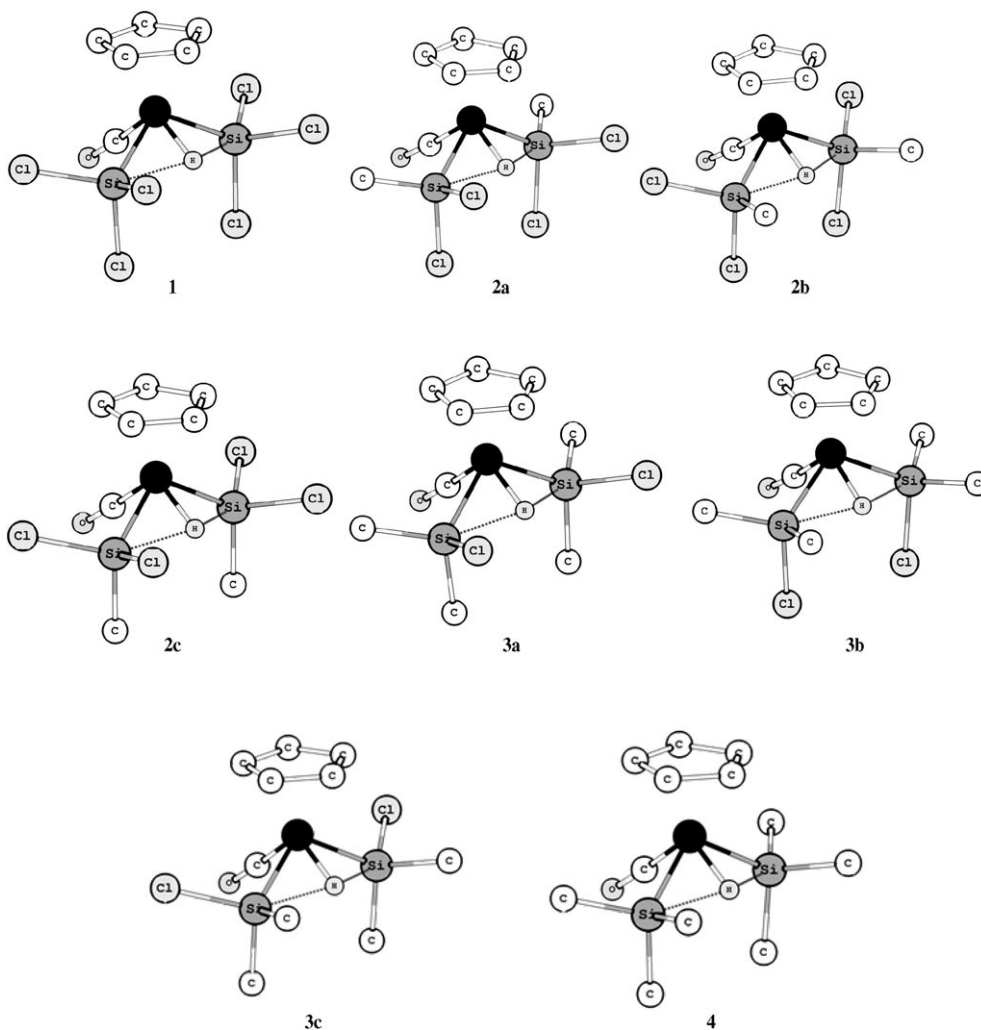


Figure 2. Structure of the carbonyl-containing bis(silyl)hydride complexes **1–4**. Dark balls denote the iron atom, white and grey balls are nonmetal atoms. Hydrogen atoms, except hydrides, are omitted for clarity. Methyl groups in silyl ligands are marked with “C”.

Table 1. Selected calculated molecular parameters in complexes **1–4**.

	Distances [Å]			Si–Cl distance [Å]			Si–Fe–H–Si dihedral [°]	H–Fe–CO	Angles ^[a] [°]		
	Si–H	Fe–Si	Fe–H	<i>trans</i>	down	up			Si–Fe–CO	Ct–Fe–CO	Ct–Fe–Si
1	2.030	2.280	1.523	2.105	2.075	2.097	149.2	105.8	84.9	126.6	118.8
2a	2.053	2.302	1.520	–	2.096	2.120	149.8	104.4	84.2	127.9	118.5
2b	2.036	2.301	1.521	2.128	2.097	–	151.8	104.1	85.2	126.8	118.4
2c	2.036	2.295	1.521	2.125	–	2.119	146.7	105.0	83.5	128.0	119.7
3a	2.065	2.325	1.515	–	–	2.144	145.8	104.0	82.5	129.5	119.8
3b	2.055	2.331	1.515	–	2.121	–	153.2	102.2	84.7	128.3	118.1
3c	2.046	2.324	1.522	2.151	–	–	149.5	103.3	83.9	128.0	119.3
4	2.075	2.361	1.514	–	–	–	149.6	103.3	83.9	129.9	119.2

[a] “Ct” denotes the centroid of the five carbon atoms of the cyclopentadienyl ring.

tational isomers. For the sake of simplicity, we calculated only three possible rotamers denoted by symbols **a–c** (their exact configuration is clear from Figure 2), in which both silyl groups are oriented in the same fashion (for the relative energy of isomers **a–c** see Table S11 in the Supporting Information). Although no symmetry constraints were imposed, all the calculated structures converged to nearly symmetric C_s geometries that were confirmed by force-constant matrix calculations to be true minima on the potential-energy surface (PES). All attempts to optimize an asymmetric structure with different Si–H distances led to the symmetric geometry. The calculated complex **1** is an exact model of the real compound $[\text{Fe}(\text{Cp})(\text{OC})(\text{SiCl}_3)_2\text{H}]$, for which X-ray structure is available^[24] and can be used to assess the quality of our calculations. A very good agreement is found between the observed and calculated geometries, which underpins the applicability of the chosen level of theory.

The bonding in piano-stool complexes $[\text{M}(\text{Cp})(\text{L})_4]$ has been the subject of several theoretical studies.^[27] The orbital structure of the $\{\text{M}(\text{Cp})(\text{L})\}$ fragment is also very well known.^[28] The deviations of the Ct–M–L angles (Ct is the centroid of the Cp ring) from the ideal 135° in some $[\text{M}(\text{Cp})(\text{L})_4]$ complexes was previously discussed in terms of π interaction of ligands L with metal M^[27a,b] and non-equivalent σ interactions of L with M,^[27d] this allows for the optimization of metal–ligand bonding. The most intriguing structural feature of complexes **1–4** is that there is another type of distortion from the ideal square-pyramidal geometry. Namely, the silyl groups approach the hydride ligand in such a way that there is a tendency to flatten the $\{\text{FeSi}_2\text{H}\}$ fragment. For example, in **1** the Si–Fe–H–Si dihedral angle is about 147.5° as compared with the dihedral angle Si–Fe–C–Si of 115.5° . Thus, the hydride deviates only slightly from the Si–Fe–Si plane (Figure 3). As seen from Figure 3, the two silyl ligands are clearly shifted to the hydride ligand. As a result, the Si–Fe–H bond angles are noticeably smaller than the OC–Fe–Si bond angles (in **1**, 60.7° versus 84.5° , respectively). Such a distortion is at odds with the previously discussed models,^[27b] because it diminishes the overlap between the silicon and metal orbitals.

Which factor is responsible for this distortion? Sterics does appear to be essential, taking into account that the calculated OC–Si distance in **1** of 2.752 \AA is much smaller than the sum of the van der Waals radii (3.85 \AA). Although this silyl shift brings the silyl group to a closer proximity to the Cp ring, the shortest SiCl_3 –Cp contact in **1**, a Cl–H contact of 3.068 \AA , is quite comparable with the sum of van der Waals radii (3.1 \AA). On the other hand, the resultant Si–H distances (2.030 – 2.075 \AA) are much smaller than the sum of the van der Waals radii (3.2 \AA), suggesting that an attractive interaction can exist between the silyl and hydride ligands.

Whatever is the cause or the effect of this distortion, it allows for an alternative description of complexes $[\text{Fe}(\text{Cp})(\text{OC})\text{Fe}(\text{SiR}_3)_2\text{H}]$ as edge-bridged pseudo-octahedral compounds (Figure 1), rather than piano-stool complexes. This view is based on the known isobal relationship of the Cp^- ligand to a set of three facial L ligands.^[29] The fragment

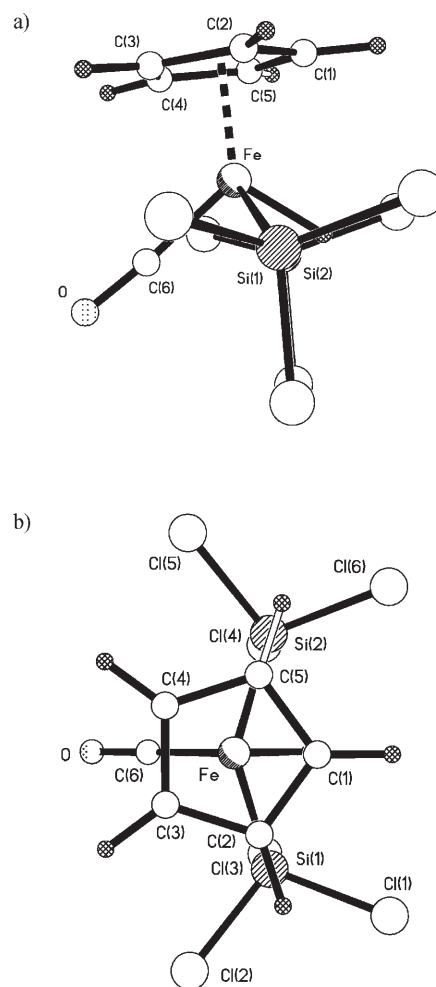


Figure 3. a) A side-on view on complex $[\text{Fe}(\text{Cp})(\text{OC})(\text{SiCl}_3)_2\text{H}]$ (**1**) and b) a view down the Ct–Fe vector on the same complex, showing the shift of silyl ligands towards the hydride.

$[\text{Fe}(\text{Cp})(\text{CO})]^+$ can be considered then as derived by removing two *cis* ligands L from a pseudo-octahedral structure $[\text{Fe}(\text{Cp})(\text{CO})(\text{L})_2]^+$. The validity of this approach is proved by the calculation of the Ct–Fe–CO bond angles in **1–4** (range 126.0 – 129.9°), which are in good agreement with the ideal value of 123.3° , obtained by assuming that the Cp ligand occupies the center of an octahedral facet. For example, the calculated angle Ct–Fe–CO for **1** of 126.6° is close to the experimental values for complexes $[\text{Fe}(\text{Cp})(\text{OC})(\text{SiR}_3)_2\text{H}]$ (range 125.5 – 128.5°)^[24–26] As shown in Figure 1, at such a bond angle, the π^* orbitals of CO find excellent overlap with two metal-centered electron pairs amenable for π back-donation. The presence of a distorted pseudo-octahedral environment is further supported by the proximity of the OC–Fe–Si bond angles to the ideal value of 90° . For example, in **1** the calculated bond angle OC–Fe–Si is 84.6° , very close to the experimental values of $85.1(3)^\circ$ and $84.4(3)^\circ$.

Consider now the MO interaction diagram for the complexation of a disilylhydride ligand $(\text{R}_3\text{Si-H-SiR}_3)^-$ to the fragment $[\text{Fe}(\text{Cp})(\text{CO})]^+$ (Figure 1). The electronic structure

of the ligand $(R_3Si-H-SiR_3)^-$ is analogous to that of the well-studied H_3^- , except that the less electronegative silicon atoms contribute less to the lowest totally symmetric ligand MO ψ_1 , but are the main contributors to the antibonding orbital ψ_3 .^[29c] The hydrogen atom bridges the Si–Si edge of the complex close to the $FeSi_2$ plane, because it is in this geometry that the occupied ligand orbital finds the best match with the fragment orbital $2a'$ (local C_s symmetry is assumed), which leads to the formation of a four-center two-electron bond. Another occupied ligand orbital, ψ_2 , overlaps well with the metal-centered orbital a'' . The HOMO of the fragment $\{Fe(Cp)(CO)\}^+$, $1a'$, is a high-lying nonbonding orbital not involved in the π -conjugation with the CO-ligand and amenable, in principle, for back-donation to the $(R_3Si-H-SiR_3)^-$ ligand (Figure 1).

Is there a possibility for retaining some Si–H bonding upon coordination of $(R_3Si-H-SiR_3)^-$ to $[Cp(CO)FeL_2]^+$? The donations $\psi_1 \rightarrow 2a'$ and $\psi_2 \rightarrow a''$ cannot break the Si–H bond completely, but the back-donation from $1a'$ to the Si–H antibonding orbital can. However, one can see that this back-donation cannot be effective enough, firstly, because the metal d orbital $1a'$ has a semi-core character (contracted due to the fact that iron is a first transition row element) and because it finds a poor overlap with the silicon-based ψ_3 . It is the little contribution of hydrogen to the central part of ψ_3 , stemming from the difference in electronegativity between hydrogen and silicon,^[29c] which impairs the overlap of ψ_3 with $1a'$. The π -acceptor carbonyl ligand in **1–4** affects the H–Si interactions only indirectly, because the metal “nonbonding” d orbitals, involved in the π -conjugation with CO, are orthogonal to the $FeSi_2H$ plane and do not overlap with the frontier orbitals of $(R_3Si-H-SiR_3)^-$.

Therefore, such structural partitioning of $[Fe(Cp)(OC)(SiR_3)_2H]$ into the $\{Fe(Cp)(OC)\}^+$ and $(R_3Si-H-SiR_3)^-$ fragments accounts well for the observed distortion of the compounds $[Fe(Cp)(OC)(SiR_3)_2H]$ from the ideal piano-stool geometry.

DFT calculation of bis(silyl)–carbonyl complexes $[Fe(Cp)(OC)(SiMe_nCl_{3-n})_2H]$ —further structural features: All previously described types of nonclassical Si–H interactions are very sensitive towards the substitution at silicon atom.^[8] For example, in complexes with interligand hypervalent interactions (IHI),^[30] the Si–H bonding is the strongest when there is only one electron-withdrawing group X at silicon oriented *trans* to the hydride. IHI leads to elongated Si–X bonds, shortened M–Si bonds, and elongated M–Si bonds. It follows from Table 1 that, generally speaking, the Fe–Si bond elongates and the Si–Cl bonds contract from **1** to **4**. These are known trends, consistent with increasing silicon p character in the Fe–Si bond and hence increasing silicon s character in the Si–Cl bond, when the number of accepting groups at silicon decreases.^[31] However, there is only marginal and rather irregular variation of the Fe–H bond length, which primarily depends on the choice of the rotamer **a**, **b**, or **c** in the case of complexes **2** and **3**, rather than on the number of chlorine atoms at silicon. The variation of

Si–H contact also primarily depends on the rotamer **a–c**. The shortest Si–H bond is found for the more chlorinated silyls **1** and **2**, which suggests the absence of IHI in these complexes.

To elucidate the bonding situation in complexes **1–4**, we calculated the Mayer bond order (MBO)^[14] and the Wiberg bond order (WBO)^[15] (Table 2). The MBOs for the Si–H

Table 2. Mayer bond orders (MBO) and Wiberg bond orders (WBO) for the Si–H and Si–Cl bonds.

	Si–H MBO		Si–H WBO PBE/PBE/ normal basis	Si–Cl MBO		
	PBE/PBE/ normal basis	B3LYP/ de-IGLO-III-ext		<i>trans</i>	<i>down</i>	<i>up</i>
1	0.138	0.180	0.2056	0.914	0.978	0.916
2a	0.142	0.192	0.2080	–	0.975	0.910
2b	0.131	0.149	0.2038	0.905	0.972	–
2c	0.137	0.170	0.2044	0.923	–	0.920
3a	0.139	0.170	0.2034	–	–	0.921
3b	0.132	0.162	0.2068	–	0.982	–
3c	0.130	0.146	0.2033	0.918	–	–
4	0.132	0.146	0.2024	–	–	–

contacts were found in the range 0.146–0.192, with the largest value observed for the dichlorosilyl complex **2a**. The corresponding WBOs vary in a very narrow range 0.202–0.208, again with the largest value found for **2a**. Surprisingly, among three possible rotamers of **2**, **2a** is the compound with the longest Si–H contact. Such significant values for MBOs and WBOs are unambiguously indicative of some bonding between the hydride and silyl ligands, which is surprisingly insensitive of the nature of the silyl ligand and its orientation relatively the Fe–H bond. It should be noted that the MBO does not directly depend on the interatomic overlap and, therefore, longer interatomic distances with the same MBO indicate an energetically *weaker* interaction. To rule out the possibility of a high MBO resulting from some sort of a three-center bonding, we evaluated three-center bond indices^[16] for the Fe–Si–H triangle, but found no values exceeding 0.04. Other known types of nonclassical interligand Si–H bonding, such as those in silane σ -complexes^[6b,8,10,32] and in compounds with IHI^[8,30] strongly depend on the number of accepting groups at silicon. In addition, the IHI is very sensitive to the relative orientation of the M–H and Si–X bonds.^[8,30g]

Thus, the trends observed for **1–4** are consistent with the presence of a distorted $(R_3Si-H-SiR_3)^-$ ligand, although a clear-cut evidence is missing. Similarly complicated interligand Si–H bonding, which is neither pure silane Si–H σ complexation nor IHI, has been previously observed in some ruthenium complexes with secondary interactions between silicon and hydrogen atoms (SISHA).^[9c–h]

DFT calculations of bis(silyl)–phosphine complexes $[Fe(Cp)(Me_3P)(SiMe_nCl_{3-n})_2H]$: To establish the effect of ligand environment on the extent and type of the Si–H interaction, we calculated a series of PMe_3 -containing complexes **5–8** (Figure 4, Table 3). Such compounds, lacking a π -

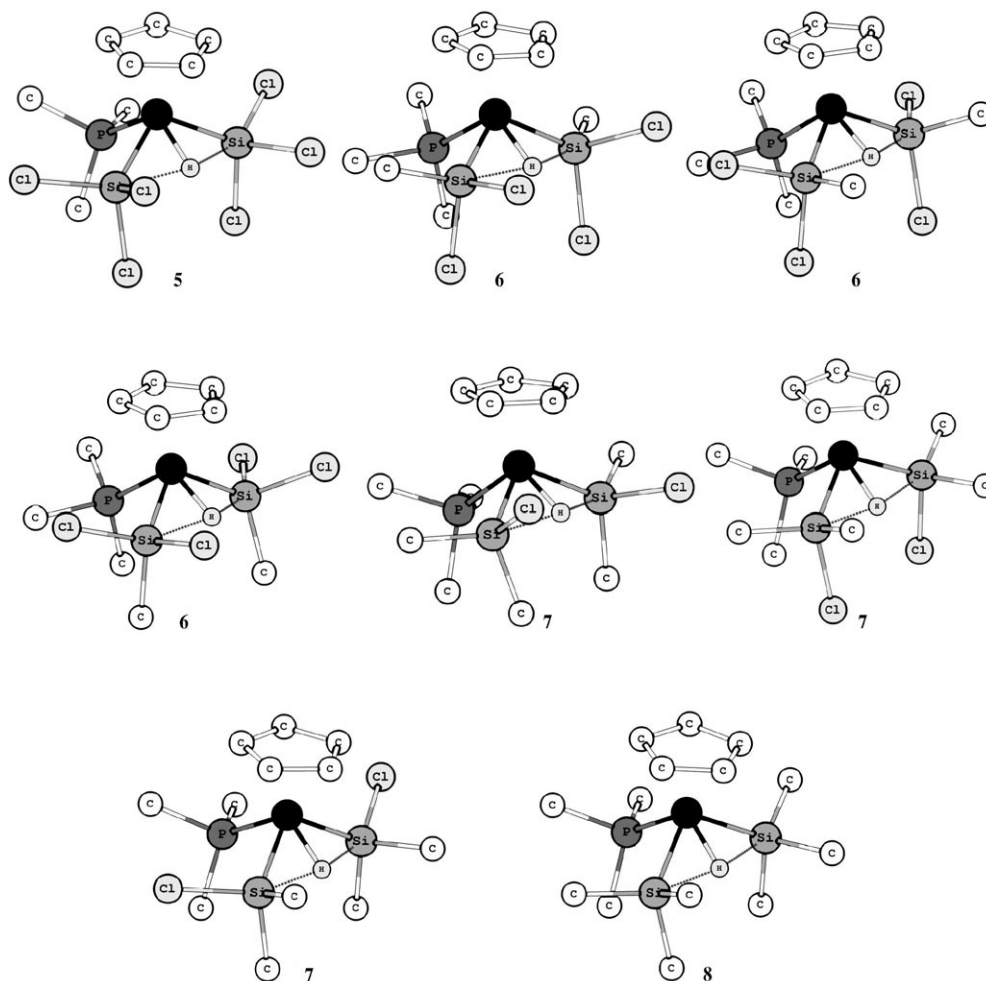


Figure 4. Structure of the trimethylphosphine-containing bis(silyl)hydride complexes **5–8**. Notations are the same as in Figure 2.

Table 3. Selected calculated molecular parameters in complexes **5–8**. Notations are the same as in Table 1.

	Distances [Å]		Fe–Si		Fe–H	<i>trans</i>	Si–Cl distance [Å]		Si–Fe–H–Si dihedral [°]	H–Fe–P	Angles [°]		
	Si–H						down	up			Si–Fe–P	Ct–Fe–P	Ct–Fe–Si
5	1.972	1.943	2.269	2.275	1.524	2.131/2.133	2.106/2.099	2.109/2.112	157.3	109.8	91.1/91.3	123.6	116.5/116.9
6a	1.997	1.946	2.294	2.304	1.520	–	2.132/2.122	2.133/2.137	161.6	106.6	91.4/91.1	125.2	116.2/115.4
6b	1.961	1.944	2.294	2.295	1.524	2.156/2.154	2.128/2.128	–	161.9	107.7	91.8/92.6	123.2	116.1/116.5
6c	1.960	1.942	2.288	2.298	1.522	2.152/2.155	–	2.136/2.139	156.4	109.5	90.6/91.5	123.6	117.6/117.4
7a	1.981	1.969	2.321	2.337	1.514	–	–	2.167/2.166	158.1	107.5	90.3/91.0	125.4	116.6/117.3
7b	1.984	1.947	2.328	2.333	1.517	–	2.160/2.156	–	170.0	102.5	92.9/92.5	125.5	115.0/114.7
7c	1.954	1.937	2.324	2.329	1.524	2.180/2.179	–	–	163.3	106.2	92.7/91.8	123.7	116.7/116.9
8	1.996	1.955	2.365	2.379	1.516	–	–	–	165.9	103.5	91.7/91.9	125.6	116.3/116.3

acceptor ligand, possess a significantly electron-rich metal centre. Similarly to the isostructural carbonyl complexes **1–4**, complexes **5–8** are best viewed as having edge-bridged distorted octahedral geometry, with the P–Fe–Si bond angles close to 90° (calculated range 90.3–92.9°). Compared to **1–4**, the Si–H distance is significantly shorter in the phosphine derivatives **5–8**. Moreover, phosphine complexes are asymmetric, with one Si–H distance being longer than the other. This result is at odds with the common expectation that the substitution of a π -acceptor ligand, such as carbonyl, for a σ -donor ligand, such as PMe_3 , should decrease the extent of

Si–H interaction.^[6b] However, inspection of Figure 1 shows that the π -accepting effect is not important in this system. The metal-centered lone-pairs are approximately orthogonal to the FeSi_2H mean plane, and their delocalization onto the L ligand does not affect much the extent of the Si–H interaction. The only fragment $\{\text{Fe}(\text{Cp})(\text{L})\}$ orbital that depends on L is $2a'$, which is antibonding with regard to L but can mix with the totally symmetric ψ_1 orbital of the ligand $(\text{R}_3\text{Si-H-SiR}_3)^-$. Since both CO and PMe_3 are good σ donors, it is hard to rationalize how this substitution leads to the strengthening of the Si–H interaction in **5–8**.

Compared with carbonyl analogues **1–4**, there is further flattening of the FeSi₂H moiety in complexes **5–8** such that the Si–Fe–H–Si dihedral angle increases to 157.3–165.9°, with more methyl-substituted silyl group tending to have the hydride closer to the FeSi₂ plane.

The Fe–Si bond length varies broadly and increases noticeably with increasing methyl substitution in the silyl ligand. There is no correlation between the Fe–Si bond length and the corresponding Si–H distance. However, for a given complex, the silyl ligand that forms the shortest Si–H contact also forms the longest Fe–Si bond. This in contrast to the situation observed in complexes with IHI, where a shorter Si–H bond corresponds to a shorter Fe–Si bond.

The Fe–H bond length occurs in a narrow range of 1.937–2.071 Å and varies rather erratically with the number of chlorine atoms at silicon and with the orientation of the silyl with respect to the hydride ligand.

The Mayer bond orders (MBO, Table 4) for the shorter of the two non-equivalent Si–H interactions are in all cases sig-

Table 4. Mayer bond orders (MBO) for the Si–H and Si–Cl bonds (normal basis set).

	Si–H MBO		Si–Cl MBO		
		<i>trans</i>	down	up	
5	0.148	0.162	0.836/0.872	0.915/0.878	0.894/0.891
6a	0.149	0.175	–	0.863/0.893	0.882/0.892
6b	0.137	0.174	0.876/0.829	0.878/0.906	–
6c	0.150	0.163	0.834/0.862	–	0.882/0.883
7a	0.139	0.142	–	–	0.916/0.907
7b	0.131	0.196	–	0.866/0.895	–
7c	0.152	0.165	0.884/0.838	–	–
8	0.148	0.180	–	–	–

nificantly higher than for the longer ones. The longer interaction exhibits MBO values closer to those discussed above for complexes **1–4**. Overall, the Si–H bonds are shorter and their MBOs are 0.03–0.04 larger than for the Si–H bonds in **1–4**.

To summarize, the bonding situation observed in complexes **5–8** is very much the same as in the compounds **1–4**. The Si–H interactions are asymmetric and stronger than in the carbonyl analogues. However, the interligand bonding in both **1–4** and **5–8** is different to what was previously observed in silane σ -complexes and compounds with IHI.

DFT calculations of mono(silyl)–hydride–methyl complexes

[Fe(Cp)(OC)(SiMe_nCl_{3–n})H(Me)]: We turned then to the study of mono(silyl) complexes of the type [Fe(Cp)(OC)(SiMe_nCl_{3–n})H(X)] to determine how the nature of the group X can affect the extent of Si–H interaction in comparison with the bis(silyl) series.

In the three-substituted systems of the type [M(L)_n(SiR₃)(H)(X)] there is a possibility of formation of two alternative nonclassical structures, that is, [M(L)_n(η^2 -HSiR₃)(X)] and [M(L)_n(SiR₃)(η^2 -HX)]. There are only few theoretical works in which the competition between the η^2 -silane versus η^2 -dihydrogen form has been addressed.^[4k,q,33] An earlier work by Lledós and Maseras on fifteen possible isomers of the compound [Os(H₃P)₂(OC)(Cl)(H₂SiR₃)] showed that both the η^2 -silane and η^2 -dihydrogen structures are plausible, with the η^2 -H₂ complex being only slightly preferred at the MP4 level of theory.^[4k] It has been concluded that silanes bind stronger to metals than hydrogen molecules due to the fact that silanes are both stronger σ donors and better π acceptors.^[4u,7] However, stronger energetics of the H–H bond can overshadow this effect, so that the preference of one form versus the other will be decided on the delicate balance of these two factors and the difference in energy of the M–H and M–Si bonds.^[4k] The same arguments apply to the competition of η^2 -H–Si versus η^2 -H–C forms. Calculations on the system [Nb(Cp)₂(SiH_nCl_{3–n})(H)(X)] (X = H or Me; n = 0–3) showed strong preference of the H–Si interactions versus the H–Me or H–H interactions,^[33] in accord with our experimental and theoretical results on [Nb(Cp)₂(SiMe₂Cl)(H)₂].^[30g]

The result of calculations of mixed silyl–hydride–methyl complexes [Fe(Cp)(OC)(SiMe_nCl_{3–n})H(Me)] (**9–12**, n = 0–3; Figure 5) are given in Table 5 (geometrical parameters) and Table 6 (Mayer bond orders). All the complexes exhibit very short Si–H separations that fall within the range of 1.822–1.856 Å. Correspondingly, the Si–H Mayer bond orders are very high (0.2 and more). On the whole, the MBOs have a clear trend to increase with decreasing Si–H separation, with **11b** being the only exception (short distance, but rather low bond order). As in the systems discussed above, the Fe–Si bond length becomes longer with increasing methyl substitution in the silyl ligand (**9** < **10** < **11** < **12**), in accordance with Bent's rule.^[31] In spite of the increase of the Fe–Si separation, the Si–H bond tends to shorten from **9** to **12** but in a rather irregular manner, de-

Table 5. Selected calculated molecular parameters in complexes **9–12**. Notations are the same as in Table 1.

	Distances [Å]					Si–Cl distance [Å]			Angles [°]				
	Si–H	Fe–Si	Fe–H	Fe–CH ₃	H–CH ₃	<i>trans</i>	down	up	H–Fe–CO	Si–Fe–CO	Ct–Fe–CO	Ct–Fe–Si	Ct–Fe–Me
9	1.856	2.246	1.511	2.084	2.001	2.112	2.092	2.106	107.4	84.6	127.4	121.8	119.4
10a	1.834	2.280	1.511	2.078	2.019	–	2.114	2.127	106.9	83.2	128.0	122.3	119.6
10b	1.848	2.278	1.512	2.078	2.029	2.135	2.113	–	106.2	84.4	127.5	120.9	119.4
10c	1.852	2.278	1.512	2.079	2.051	2.135	–	2.127	106.0	83.2	128.6	121.2	118.8
11a	1.836	2.323	1.509	2.073	2.071	–	–	2.149	106.4	81.5	129.0	122.4	119.5
11b	1.826	2.327	1.509	2.073	2.050	–	2.137	–	105.6	83.1	128.3	121.5	119.7
11c	1.844	2.323	1.514	2.073	2.084	2.160	–	–	105.2	82.8	128.3	120.8	119.0
12	1.822	2.385	1.512	2.068	2.103	–	–	–	105.3	81.1	129.0	122.3	119.7

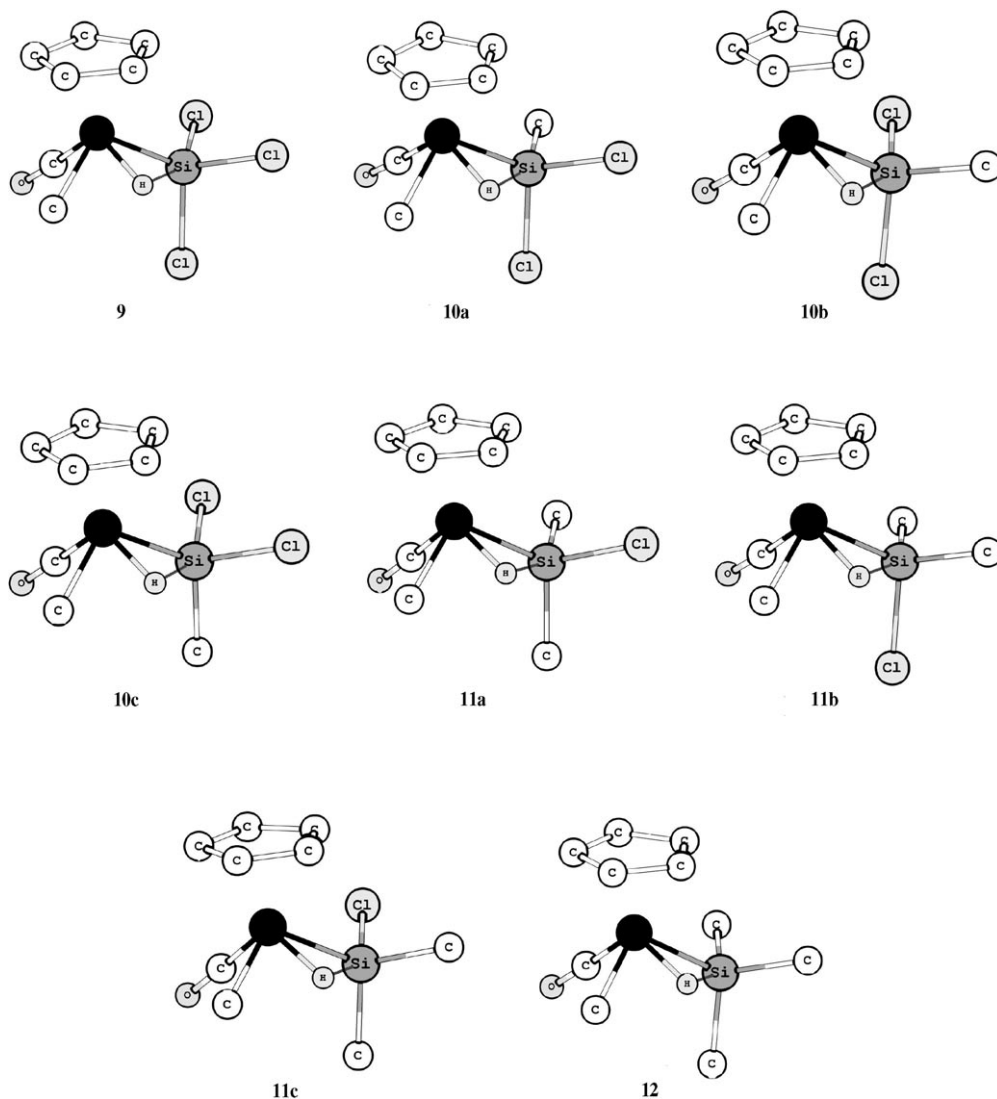


Figure 5. Structure of the methyl-containing silyl-hydride complexes **9–12**. Notations are the same as in Figure 2.

Table 6. Mayer bond orders (MBO) for the Si–H and Si–Cl bonds in **9–12** (normal basis set).

	MBO			Si–Cl MBO		
	Si–H	H–CH ₃	<i>trans</i>	<i>down</i>	<i>up</i>	
9	0.218	0.067	0.902	0.933	0.889	
10a	0.246	0.063	–	0.928	0.885	
10b	0.218	0.060	0.891	0.931	–	
10c	0.220	0.059	0.900	–	0.894	
11a	0.242	0.056	–	–	0.893	
11b	0.193	0.057	–	0.929	–	
11c	0.220	0.052	0.899	–	–	
12	0.246	0.048	–	–	–	

pending on the rotamer of complexes **10** and **11** (see Table S13 in the Supporting Information for the relative stability of the rotamers **a–c**). This trend indicates that electron-releasing groups at silicon strengthen the Si–H interaction, a behavior typical of silane σ -complexes.

Compared to the Si–H distances, the C–H distances are noticeably longer, despite the fact that the Fe–C bond is much shorter than the Fe–Si bond. These C–H distances correspond to small MBOs of 0.06–0.07, which is virtually nonbonding. Such a situation emerges as a result of hydrogen atom shift in the coordination sphere of iron to the silicon atom, away from the carbon atom.

There is no explicit shortening of the Fe–Si bond corresponding to the long Si–Cl bond in the different rotamers of complexes **10** and **11**. This is in contrast to the situation found for compounds with IHI.^[30] Further supporting the absence of IHI is the observation that the largest MBOs for the Si–H interactions are in compounds with a Me group *trans* to the hydride (Table 6).

In total, these structural and bonding features of **9–12** are consistent with their preferred description as silane σ -complexes $[\text{Fe}(\text{Cp})(\text{OC})(\eta^2\text{-H-SiMe}_n\text{Cl}_{3-n})(\text{Me})]$.^[7,8,10,32] The same conclusion has been reached for the related cationic complex $[\text{Fe}(\text{Cp})(\text{OC})(\text{H}_3\text{P})(\eta^2\text{-H-SiH}_3)]^+$.^[34]

Can a qualitative MO diagram, similar to that in Figure 1, account for this result? The answer is that it can. The main difference between the putative ligand $(R_3Si-H-CH_3)^-$ and $(R_3Si-H-SiR_3)^-$ is that in the former the most electronegative atom C is the main contributor to the lowest orbital ψ_1 , leading to more H and Si character in the higher lying orbitals ψ_2 and ψ_3 . As the result, the interaction of a' with ψ_1 leads to the formation of a strong Fe–C bond, whereas an incomplete back-donation on ψ_3 results in the formation of a $\eta^2-H-SiR_3$ ligand.

To get further insight into the bonding situation in complexes **9–12**, we performed Bader's atom-in-molecule (AIM) study of these compounds (Table 7).^[35,36] A bond critical

Table 7. Results of the Bader analysis for the H–Si bond in the complexes **9–12**.^[a]

	$\rho(\mathbf{r}_c)$	$\nabla^2\rho(\mathbf{r}_c)$	$H(\mathbf{r}_c)$	ϵ	$ \mathbf{r}_c-H / \mathbf{r}_c-Si $
9	0.546	–0.169	–0.206	4.610	0.766
10a	0.549	–0.989	–0.235	1.231	0.808
10b	0.535	–0.480	–0.211	2.855	0.797
10c	0.533	–0.381	–0.207	3.690	0.793
11a	0.528	–1.116	–0.232	1.170	0.844
11b	0.532	–1.269	–0.243	0.989	0.857
11c	0.515	–0.817	–0.215	1.742	0.839
12	0.506	–1.473	–0.250	0.768	0.929

[a] The density in the $(3,-1)$ bond critical point $\rho(\mathbf{r}_c)$ is in $e\text{\AA}^{-3}$, its Laplacian $\nabla^2\rho(\mathbf{r}_c)$ is in $e\text{\AA}^{-5}$, the energy density $H(\mathbf{r}_c)$ is in Hartree \AA^{-3} , and ϵ denotes ellipticity. $|\mathbf{r}_c-H|/|\mathbf{r}_c-Si|$ is the ratio of distances from the bond critical point to the hydrogen and silicon nuclei.

point between the hydride and silyl groups was found in all the methyl complexes under discussion, thus confirming their formulation as compounds with nonclassical Si–H bonding. The Laplacian $\nabla^2\rho(\mathbf{r}_c)$ in the Si–H bond critical point is negative in all cases, but its values vary widely and correlate reasonably well with the Si–H distance (the shorter the distance, the more negative is the Laplacian). In contrast, the electron density $\rho(\mathbf{r}_c)$ does not exhibit a clear correlation with the Si–H bond length, but approximately follows the distance $|\mathbf{r}_c-H|$. In particular, the bond critical point shifts away from the hydrogen nucleus due to the influence of the silicon if the latter comes closer to the former.

Table 7 reveals a seemingly paradoxical situation in that the bond critical point approaches the hydrogen atom as the Si–H distance decreases, accompanied by the decrease of electron density $\rho(\mathbf{r}_c)$. In our opinion, the location of the Si–H bond critical point is largely determined by an interplay between the hydrogen and silicon atomic densities. In the area of a considerable overlap of the Si and H atomic densities, that is, at relatively short Si–H distances, the decay of the density from the hydrogen nucleus toward the silicon nucleus slows down as the silicon atom approaches hydrogen. Consequently, the critical point shifts away from the hydrogen (Table 7, second and sixth columns). As a result, the total electron density in the critical point decreases. In contrast, at long Si–H distances, when the overlap is small, the density between the atoms decreases with increasing Si–H

separation. Starting from some particular interatomic separation, the Si–H bond critical point collapses, and only Fe–Si and Fe–H bond paths persist. In our experience^[30g,37] this “breakdown” distance for a Si–H interaction lies at about 1.9 \AA . Consequently, the complexes **9–12** with short Si–H distance exhibit well-defined Si–H critical points, whereas all other complexes under study with longer Si–H separations (**1–8**) do not. This consideration shows that the presence of a bond critical point in the case of the Si–H interactions depends directly on the Si–H distance, and its absence does not mean the absence of any interaction.

DFT calculations of mono(silyl) dihydride complexes

[Fe(Cp)(OC)(SiMe_nCl_{3–n})H₂]: To establish a possible competition of the H–Si versus H–H interactions^[48] we have calculated a series of bis(hydride) complexes $[\text{Fe}(\text{Cp})(\text{OC})(\text{SiMe}_n\text{Cl}_{3-n})\text{H}_2]$ (**13–16**, $n=0-3$) (Figure 6). Selected geometric parameters and Mayer bond orders are summarized in Tables 8 and 9, respectively. Compared with **1–4**, the substitution of one lateral silyl for a hydride has a profound effect on the structure of these monosilyl hydride complexes. In particular, either a $\eta^2-(\text{H}-\text{H})$ or a $\eta^2-(\text{Si}-\text{H})$ complex is formed depending on the substituents at silicon and the orientation of the silyl group relative to the central hydride. One can roughly divide complexes **13–16** into three groups, according to the extent of H–H and Si–H interactions:

Group A: Complexes **13**, **14**, **15a-2**, and **15b** can be classified as dihydrogen complexes with an H–H distance of ~ 1 \AA , an H–H MBO of ~ 0.3 , very large Si–H separations of ~ 2.25 \AA , and small corresponding Si–H MBOs of $\sim 0.07-0.08$. They should be considered as typical dihydrogen complexes, containing a $\eta^2-\text{H}_2$ ligand, without a significant Si–H interaction. The dihydrogen form is favored for complexes with more electron-withdrawing substituents at silicon, which can be attributed to the stabilization of the M–Si bond in the presence of electronegative substituents at silicon.

Group B: By way of contrast, complexes **15c** and **16** are better described as nonclassical bis(hydride) complexes with some Si–H interactions. In these compounds the H–H separation varies widely from 1.49 to 1.77 \AA , with the MBO decreasing correspondingly from 0.08 to 0.04. The Si–H MBO is increased and varies between 0.13 and 0.15, which is close to the values obtained for the bis(silyl) complexes discussed above, and much larger than those found for the dihydrogen complexes **13**, **14**, **15a-2**, and **15b**.

Group C: The complex **15a** is a very interesting case, since the bis(hydride) form denoted as **15a-1** coexists with its dihydrogen isomer **15a-2**, which is only 0.3 kcal·mol^{–1} less stable on the ΔG_{298}° scale. Both **15a-1** and **15a-2** are established minima on the PES, but the transition state between them lies slightly below both of them on the ΔG_{298}° scale. This means that the actually observed picture consists of an averaged structure with large-amplitude highly anharmonic

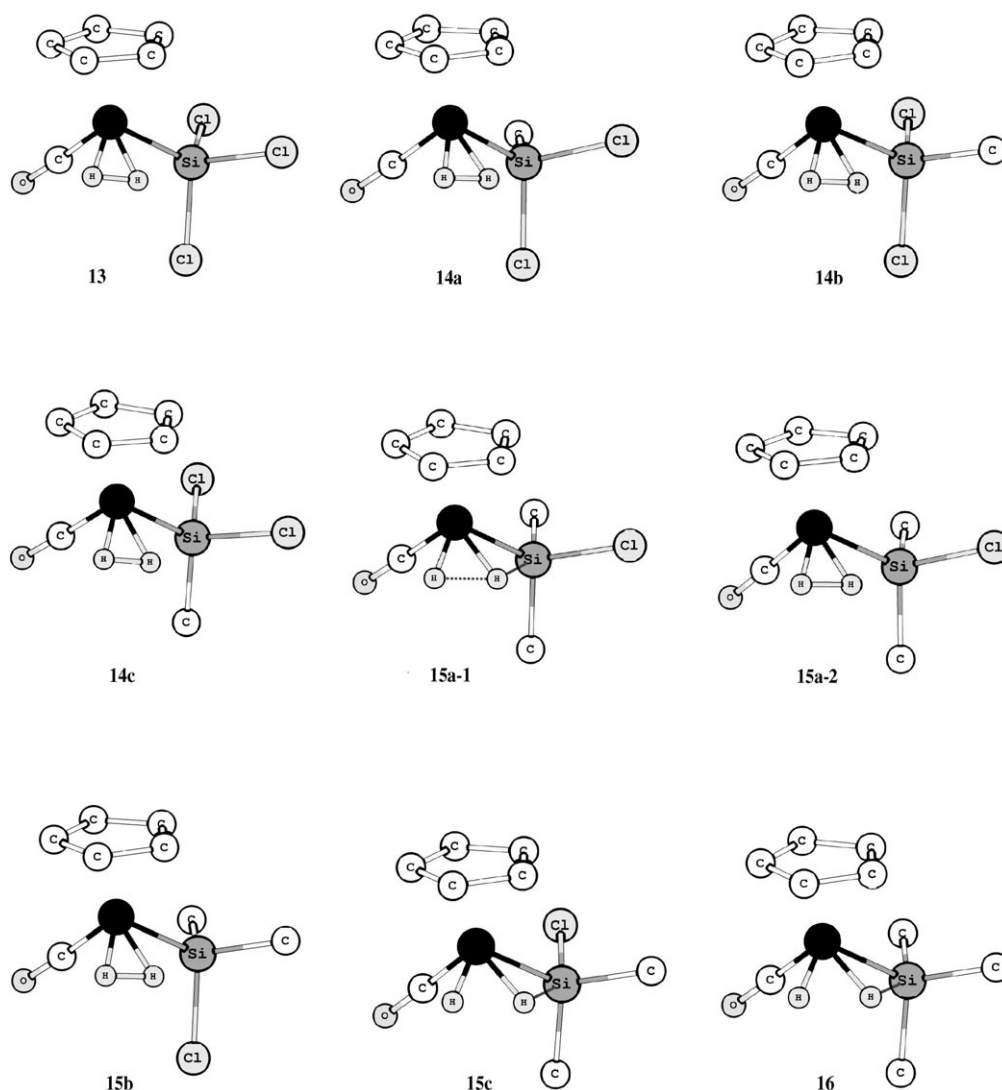


Figure 6. Structure of the bishydride and dihydrogen silyl complexes **13**–**16**. Notations are the same as in Figure 2.

Table 8. Selected calculated molecular parameters in complexes **13**–**16**. Notations are the same as in Table 1.^[a]

	Distances [Å]					Si–Cl distance [Å]			Angles [°]			
	Si–H	Fe–Si	Fe–H ^l	Fe–H ^a	H–H	<i>trans</i>	<i>down</i>	<i>up</i>	Si–Fe–CO	Ct–Fe–CO	Ct–Fe–Si	Ct–Fe–H ^l
13	2.281	2.246	1.551	1.545	0.982	2.109	2.100	2.114	87.3	127.8	122.2	120.5
14a	2.271	2.270	1.547	1.543	0.990	–	2.121	2.135	85.9	128.5	122.5	121.1
14b	2.246	2.269	1.540	1.534	1.020	2.130	2.120	–	86.9	128.3	121.7	120.9
14c	2.248	2.269	1.538	1.532	1.030	2.130	–	2.133	85.7	129.0	122.3	120.0
15a-2	2.236	2.301	1.530	1.526	1.055	–	–	2.155	83.8	130.9	123.2	118.7
15b	2.237	2.304	1.535	1.531	1.031	–	2.145	–	85.5	130.0	122.7	120.7
15a-1	2.041	2.304	1.503	1.494	1.362	–	–	2.151	83.4	129.1	122.0	121.4
15c	1.979	2.307	1.507	1.491	1.483	2.156	–	–	84.6	130.3	122.3	117.8
16	1.954	2.359	1.503	1.491	1.523	–	–	–	82.8	131.3	122.9	118.4

[a] H^l is the hydrogen atom remote from silyl, H^a is adjacent to the silyl.

vibrations. Nevertheless, we shall discuss **15a-1** and **15a-2** separately, as we are interested mostly in the electronic structure of the complexes.

The isomer **15a-1** is unique, since both a short Si–H distance of 2.041 Å with the corresponding MBO of 0.133 and a shortened H–H distance of 1.36 Å with a significant MBO

of 0.129 are found. The central hydride atom involved into nonclassical bonding both with the silicon and lateral hydride center exhibits a slightly longer Fe–H bond of 1.503, compared to the Fe–H^{lateral} bond of 1.494 Å. This situation is similar to that observed in hydride(dihydrogen) complexes with the *cis* effect, in which the dihydrogen atom tilts in

Table 9. Si–H, H–H, and Si–Cl Mayer bond orders (MBO) in complexes **13–16** (normal basis set).

	MBO		Si–Cl MBO		
	Si–H	H–H	<i>trans</i>	down	up
13	0.068	0.344	0.904	0.915	0.884
14a	0.073	0.346	–	0.905	0.872
14b	0.077	0.309	0.891	0.900	–
14c	0.074	0.305	0.899	–	0.883
15a-1	0.133	0.129	–	–	0.888
15a-2	0.077	0.295	–	–	0.878
15b	0.082	0.307	–	0.906	–
15c	0.151	0.083	0.895	–	–
16	0.141	0.038	–	–	–

such a way that the M–H distance to the hydrogen atom closest to the hydride is the longest.^[38]

Complexes with such large H–H separations as in **15a-1** (1.2–1.4 Å), which is neither definitely bonding nor non-bonding, are called elongated (or stretched) dihydrogen complexes.^[39] Bonding in these very unusual molecules is currently subject to debate. To the best of our knowledge, complex **15a-1** is the first example of such a double interaction of a hydride ligand with another hydride and a silyl group. It can be considered as a very stretched (Si–H–H)[–] ligand frozen in the midway of transformation from the (H)–(HSiR₃) ligand set into the (H₂)(SiR₃) ligand set.

Among complexes **15**, the isomer **15c** with chlorine in the *trans* position to the hydride is the most stable (Table SI4) and has the shortest Si–H distance corresponding to the largest Si–H MBO. Although the Si–Cl *trans* bond is the longest among three possible orientations, it does not correspond to the shortest Fe–Si bond in the SiMe₂Cl series. We therefore conclude that IHI is not present in this system and bonding between the silyl and hydride ligands is better described as electron deficient, more akin to that usually found in silane σ complexes.

The formation of H–H and Si–H interactions in this system reflects the inherent electron deficiency of these formally Fe^{IV}–carbonyl complexes.

The AIM analysis (Table 10) of complexes **13–16** reveals a H–H bond path in the case of typical dihydrogen complexes, that is, when the H–H bond length is about 1 Å. However, the bond path vanishes at larger H–H separation. As expected, the $\rho(\mathbf{r}_c)$ and $-\nabla^2\rho(\mathbf{r}_c)$ values increase with decreasing bond length. The Laplacian $\nabla^2\rho(\mathbf{r}_c)$ and the energy density $H(\mathbf{r}_c)$ ^[36] remain negative for all dihydrogen complexes, indicating an intact H–H covalent bond. The Si–H bond path has not been found for complexes **15a-1**, **15c**, and **16** because these complexes have relatively long Si–H distances (see the discussion in the previous section).

Silylhydride carbonyl complexes [Fe(Cp)(OC)(SiMe_nCl_{3-n})H(X)] (X=H, Me, SiMe_nCl_{3-n})—NMR properties: NMR spectroscopy and, in particular, the measurements of H–Si coupling constants $J(\text{H,Si})$ traditionally played a central role in the characterization and interpretation of nonclassical H–Si interactions.^[8,10,32] There is a

Table 10. Results of the AIM analysis of the H²–H¹⁶ bond in complexes **13–16**.^[a]

	$\rho(\mathbf{r}_c)$	$-\nabla^2\rho(\mathbf{r}_c)$	$H(\mathbf{r}_c)$	ϵ	$ \mathbf{r}_c-\text{H}^1 / \mathbf{r}_c-\text{H}^c $
13	1.076	–8.128	–0.798	0.133	0.987
14a	1.061	–7.801	–0.779	0.143	0.986
14b	1.002	–6.547	–0.704	0.172	0.985
14c	0.985	–6.195	–0.683	0.182	0.987
15a-1	–	–	–	–	–
15a-2	0.944	–5.301	–0.629	0.222	0.987
15b	0.983	–6.139	–0.680	0.189	0.984
15c	–	–	–	–	–
16	–	–	–	–	–

[a] The density in the (3,–1) bond critical point $\rho(\mathbf{r}_c)$ is in eÅ^{–3}, its Laplacian $\nabla^2\rho(\mathbf{r}_c)$ is in eÅ^{–5}, the energy density $H(\mathbf{r}_c)$ is in Hartree Å^{–3}, and ϵ denotes the ellipticity. $|\mathbf{r}_c-\text{H}^1|/|\mathbf{r}_c-\text{H}^c|$ is the ratio of distances from the critical point to both H nuclei. Missing data indicate that no bond critical point has been found. H¹ is the hydrogen atom remote from silyl, H^c is adjacent to the silyl.

mounting interest in the calculation of ligand chemical shifts and ligand–ligand coupling constants in metal complexes, although accurate calculation of NMR parameters is not an easy task.^[40] This is particularly relevant to the case in which the element under question (such as silicon) has an unusual geometry or is involved in nonclassical bonding.^[41,42] The calculation of Si–H coupling constants in metal complexes is very rare.^[43] In this work we calculated hydride chemical shifts and the coupling constants between the hydride and silyl ligands for carbonyl complexes [Fe(Cp)(OC)(SiMe_nCl_{3-n})H(X)] (X=H, Me, SiMe_nCl_{3-n}) ($n=0-3$; Table 11).

For compounds **1–4** the hydride signals tend to shift to higher field upon increasing the number of methyl groups at silicon, although the variation is rather irregular and depends on the choice of a rotamer in the case of complexes **2** and **3**. This trend can be simply rationalized in terms of increased shielding of the proton by the increased electron density released by methyl substituents at silicon. Impor-

Table 11. Calculated hydride chemical shift, hydride–silicon coupling constant, and thermally averaged $^{\text{obs}}J(\text{H},^{29}\text{Si})$ ^[a] in complexes **1–4** and **9–12**.

	δH [ppm]	$J(\text{H},^{29}\text{Si})$ [Hz]	$^{\text{obs}}J(\text{H},^{29}\text{Si})$ [Hz]
1	–9.84	–12.2	–12.2
2a	–9.45	–29.4	+1.5
2b	–12.17	+1.9	–
2c	–11.35	+1.5	–
3a	–10.39	–14.6	–12.3
3b	–11.37	–16.5	–
3c	–13.92	+7.6	–
4	–12.57	–7.8	–7.8
9	–8.17	–47.5	–47.5
10a	–8.21	–81.6	–35.8
10b	–9.35	–32.0	–
10c	–9.19	–32.2	–
11a	–8.85	–63.3	–63.0
11b	–9.11	–65.0	–
11c	–10.66	–25.5	–
12	–10.11	–55.3	–55.3

[a] $^{\text{obs}}J(\text{H},^{29}\text{Si})$ stands for the calculated coupling constant averaged according to Boltzmann distribution.

tantly, for **1–4** the calculated $J(\text{H},\text{Si})$ constants predominantly depend on the orientation of the silyl ligand rather than on the substitution at silicon. To get meaningful estimations for the observable coupling constants, we calculated the $J(\text{H},\text{Si})$ values weighted according to the Boltzmann distribution ($^{\text{obs}}J(\text{H},\text{Si})$ in Table 11).^[44] The calculated absolute value of $|J(\text{H},\text{Si})|$ for the real compound **1** (12.2 Hz) is in a good agreement with the experimental value of 20 Hz, (the experimental sign is not available).^[22] In addition, our calculations provide the signs of the coupling constants, which were found to be negative for **1**, **3**, and **4**, although the absolute values for all coupling constants are also rather low. The sign of $J(\text{H},\text{Si})$ can serve as a more meaningful criterion for the presence of a Si–H(M) nonclassical bonding, because it shows at least the prevalence of direct one-bond H–Si coupling (expected to be negative owing to the sign of the ^{29}Si magnetogyric ratio) over the two-bond coupling (which usually gives positive contribution to the $^{\text{obs}}J(\text{H},\text{Si})$).^[30a] We found an exception for the compound **2** (small positive $^{\text{obs}}J(\text{H},\text{Si})$ in spite of significant Si–H bonding manifested by the calculated bond orders), but its small value of $^{\text{obs}}J(\text{H},\text{Si})$ lies outside the accuracy of our calculations. Such unusual trends in the hydride–silicon coupling constants are very different from the values and trends observed for both silane σ complexes and for compounds with IHI.^[8] The dependence of the computed $J(\text{H},\text{Si})$ upon a particular rotamer shows that the observed (i.e., thermally averaged) $^{\text{obs}}J(\text{H},\text{Si})$ value cannot serve as a reliable indicator of the H–Si interaction in the present case.

In all the methyl complexes **9–12**, the computed magnitude of $J(^1\text{H},^{29}\text{Si})$ is large and is strongly negative, consistent with their formulation as silane σ complexes. The magnitude of thermally averaged $^{\text{obs}}J(^1\text{H},^{29}\text{Si})$ tends to increase with increased methyl substitution at silicon, also a behavior typical of silane σ complexes. However, the variation of individual $J(^1\text{H},^{29}\text{Si})$ depends strongly on the particular conformation of the silyl group. There is no correlation between the Si–H separation or Mayer bond index and the magnitude of the coupling constant. As the rotamers of **10** and **11** differ only slightly in energy (Table SI3), it means that the conformation-averaged, that is, “observed”, coupling constant $^{\text{obs}}J(^1\text{H},^{29}\text{Si})$ is extremely sensitive to minor changes in energetics and, probably, also to environment effects.

When discussing the variation of hydride–silicon coupling constant along a series of related silane σ complexes, it should be borne in mind that the electronegativity of the substituents at silicon has a dual effect on the magnitude of $J(^1\text{H},^{29}\text{Si})$.^[45] On one hand, electropositive groups at silicon push the antibonding orbital $\sigma^*(\text{H}-\text{Si})$ higher in energy, decreasing the back-donation from metal and strengthening the Si–H bond. On the other hand, this is accompanied by the decrease of silicon s character in the Si–H bond.^[45] These two trends have opposite effects on the value of a hydride–silicon coupling constant. Therefore, the observed irregularity in the variation of $J(^1\text{H},^{29}\text{Si})$ from **9** to **12** possibly reflects a complex interplay of these two trends.

In the series of “dihydride” complexes **13–16** the dihydrogen complexes **13** and **14** have small hydride–silicon coupling constants $J(^1\text{H},^{29}\text{Si})$ (Table 12), in accord with the absence of significant Si–H interaction. In contrast, the com-

Table 12. Calculated hydride chemical shift, hydride–silicon coupling constant, and thermally averaged $^{\text{obs}}J(^1\text{H},^{29}\text{Si})$ in complexes **13–16**.^[a]

	$\delta\text{H}^{\text{l}}$ [ppm]	$\delta\text{H}^{\text{c}}$ [ppm]	$J(^1\text{H},^{29}\text{Si})$ [Hz]	$^{\text{obs}}J(^1\text{H},^{29}\text{Si})$ [Hz]	$J(^1\text{H}^{\text{c}},^1\text{H}^{\text{l}})$ [Hz]
13	–11.13	–10.52	–2.1	–2.1	211.9
14a	–10.67	–10.65	–13.1	–0.7	208.9
14b	–11.52	–10.46	+0.4		194.2
14c	–11.35	–10.01	+0.8		189.8
15a-1	–9.14	–7.11	–27.5	–18.9	67.7
15a-2	–10.60	–9.89	–9.9		180.1
15b	–10.89	–10.58	–11.2		190.1
15c	–11.19	–6.86	–9.3		31.9
16	–10.52	–7.30	–31.7	–31.7	24.6

[a] H^{c} = central hydride, H^{l} = lateral hydride.

pounds **15** and **16**, for which at least some rotamers do have Si–H interactions, exhibit negative $^{\text{obs}}J(^1\text{H},^{29}\text{Si})$ with increased magnitude. However, there is no meaningful correlation between the Si–H separation and the value of $J(\text{H},\text{Si})$. In contrast, the $J(\text{H},\text{H})$ values exhibit a nearly linear correlation with the H–H distance. It is interesting that the variation of hydride chemical shift with the substitution at silicon is opposite to that observed for complexes **1–4**. Namely, increased methyl substitution at silicon tends to leave the hydride signal almost invariant (for lateral hydride) or shifts it down-field (for the central hydride). It is noteworthy that in the series **13–16** complexes with significant H–Si interactions (**15a-1**, **15c**, and **16**), down-field-shifted hydride signals are exhibited for the central hydride relative to the lateral one. Usually complexes with nonclassical H–Si interactions exhibit up-field-shifted hydride signals.^[8]

It is worth noting that despite of the increased absolute value of $^{\text{obs}}J(^1\text{H},^{29}\text{Si})$ and large MBO, complex **16** does not exhibit a Si–H bond path in the AIM study. Since complex **16** has only electron-donating groups at silicon atom, a significant $^{\text{obs}}J(^1\text{H},^{29}\text{Si})$ of –32 Hz does indicate the presence of some H–Si interaction.^[45]

Concluding Remarks

The compound $[\text{Fe}(\text{Cp})(\text{OC})(\text{SiCl}_3)_2\text{H}]$, which for a long time served as an example of a classical silyl–hydride compound, is not classical. Rather, it exhibits peculiar interligand Si–H interactions spread over the hydride and two silyl ligands. The occurrence of these interactions is seen already from a severe distortion of $[\text{Fe}(\text{Cp})(\text{L})(\text{SiMe}_n\text{Cl}_{3-n})_2\text{H}]$ from the ideal square-pyramidal geometry and is further supported by the calculation of bond indices. The highly delocalized nature of these interactions and their little sensitivity to the substituents at silicon allows us to differentiate

them from the known σ interactions in silane σ complexes. These new $R_3Si-H-SiR_3$ interactions are also different from the interligand hypervalent interactions, since they are not affected much by the conformation of the silyl ligand and change only very little and irregularly upon the variation of substituents at silicon. Another aspect that allows us to distinguish these unique $R_3Si-H-SiR_3$ interactions in complexes $[Fe(Cp)(L)(SiMe_nCl_{3-n})_2H]$ ($n=0-3$) from the Si-H σ complexation and IHI is that they are not very sensitive to the variation of supporting ligand L. In contradiction with the theory of σ complexation, the Si-H bonding strengthens on going from $L=CO$ to $L=PMe_3$; however, this increase is not large, which is at odds with the theory of IHI.

Historically, the $J(H,Si)$ NMR coupling constants of 20 Hz measured for the compound $[Fe(Cp)(OC)(SiCl_3)_2H]$ was considered to be a border line between the classical and nonclassical complexes of the type $[M(L)_n(SiR_3)(H)]$. The formulation of nonclassical nature of $[Fe(Cp)(OC)(SiCl_3)_2H]$ now brings about the question of the validity of this criterion for the characterization of nonclassical complexes. This result and our previous work on this topic suggest that such NMR criteria are no longer applicable. The magnitude of $J(H,Si)$ coupling depends primarily on the type of nonclassical interactions.

As a tentative rationale for this novel Si-H bonding, we suggest to consider these bis(silyl) derivatives as highly stretched double Si-H σ complexes of the hypervalent ligand $(R_3Si-H-SiR_3)^-$, that is, as $[Fe(Cp)(L)(\eta^3\text{-}\{(SiMe_nCl_{3-n})_2H\})]$, but other interpretations can be invoked. Whatever the most appropriate description is, the question remains open whether the structural distortions are the cause or the effect of interligand interactions.

Another question is pertinent: Why does this hydride ligand in **1-4** like to be involved in a "double" interaction with two silyl ligands, such as in the postulated ligand $(R_3Si-H-SiR_3)^-$, instead of forming a more common $[M(L)_n(SiR_3)(\eta^2\text{-}H-SiR_3)]$ structure? We do not have a clear-cut answer to this question. It could be just a steric result, stemming from the small size of the iron center. Alternatively, it may reflect an intrinsic electronic preference of silicon to be hypervalent. In this regard, it is interesting to note that there is no unequivocal example of a $[M(L)_n(H)(\eta^2\text{-}H-SiR_3)]$ or $[M(L)_n(SiR_3)(\eta^2\text{-}H-SiR_3)]$ complex without "secondary" interaction between the η^2 -silane and hydride or between the η^2 -silane and silyl ligand, respectively.^[46]

Our attempt to correlate the occurrence of interligand interactions in the family $[Fe(Cp)(L)(SiMe_nCl_{3-n})_2H]$ ($L=CO, PMe_3; n=0-3$) with the $J(H,Si)$ NMR coupling constants ended up in an unexpected observation that the magnitude of $J(H,Si)$ primarily depends on the orientation of the silyl group rather than on the number of electron-withdrawing groups at silicon. This fact again demarcates these unique Si-H interactions from those found in silane σ -complexes and nonclassical silylhydrides with IHI. In most cases, $J(H,Si)$ was calculated to be negative, which suggests that the direct one-bond component $^1J(H,Si)$ dominates over two-bond coupling $^2J(H,Si)$. However, no correlation has

been found between the magnitude of $J(H,Si)$ and the bond indices.

For the related compounds $[Fe(Cp)(OC)(SiMe_nCl_{3-n})H(X)]$ ($X=H, Me; n=0-3$) a clearer bonding picture emerged. Complexes $[Fe(Cp)(OC)(SiMe_nCl_{3-n})H(Me)]$ ($n=0-3$) should be classified as silane Si-H σ complexes $[Fe(Cp)(OC)(\eta^2\text{-}H-SiMe_nCl_{3-n})(Me)]$ for all n . The "dihydride" complexes $[Fe(Cp)(OC)(SiMe_nCl_{3-n})H_2]$ ($n=0-3$) are genuine dihydrogen complexes for $n=0$ and 1, but for $n=3$ the Si-H interaction strongly dominates over the H-H bonding. The monochlorine complex $[Fe(Cp)(OC)(SiMe_2Cl)H_2]$ presents an intermediate situation when both a dihydrogen form $[Fe(Cp)(OC)(SiMe_nCl_{3-n})(\eta^2\text{-}H_2)]$ and an isomer with simultaneous stretched Si-H and H-H interactions are present, depending on the orientation of the silyl group relative to the rest of the complex. As the energy difference between different forms is small, rather weak interligand bonding with a shallow, highly anharmonic PES must be present. The observation of nonclassical interligand interactions in $[Fe(Cp)(OC)(SiMe_nCl_{3-n})H(X)]$ ($X=H, Me; n=0-3$) provides an additional argument in favor of nonclassical nature of the related complexes $[Fe(Cp)(L)(SiMe_nCl_{3-n})_2H]$ ($L=CO, PMe_3; n=0-3$).

As previously observed in other nonclassical systems, the AIM analysis finds a Si-H bond path in complexes when the Si-H distance is less than about 1.9 Å. At longer distances, the Si-H bond path collapses into the M-H and M-Si bonds even when significant Mayer bond indices are found.

The overall conclusion is that the $\{Fe(Cp)(L)\}$ ($L=CO$ or Me_3P) platform can support a plethora of nonclassical interligand interactions. Our results suggest that activation of Si-H and H-H bonds by transition-metal complexes may involve more extended interligand interactions than have been previously anticipated and that the nature of these interactions reflects a complex balance of steric and electronic effects.

Acknowledgements

This work was supported by the Spanish Ministry of Education and Science (Ramón y Cajal Program) and Brock University.

- [1] R. H. Crabtree, *The Organometallic Chemistry of the Transition Metals*, 3rd ed, Wiley, Oxford, **2001**.
- [2] F. Maseras, A. Lledós, E. Clot, O. Eisenstein, *Chem. Rev.* **2000**, *100*, 601.
- [3] a) J.-Y. Saillard, R. Hoffmann, *J. Am. Chem. Soc.* **1984**, *106*, 2006; b) O. Eisenstein, Y. Jean, *J. Am. Chem. Soc.* **1985**, *107*, 1177; c) for a review on C-H activation, including extensive citation of theoretical work: C. Hall, R. N. Perutz, *Chem. Rev.* **1996**, *96*, 3125; d) recent review on C-H-M agostic complexes: E. Clot, O. Eisenstein, *Struct. Bonding (Berlin)* **2004**, *113*, 1.
- [4] Selected examples: a) M. Besora, F. Maseras, A. Lledós, O. Eisenstein, *Inorg. Chem.* **2002**, *41*, 7105; b) L. Perrin, L. Maron, O. Eisenstein, *Inorg. Chem.* **2002**, *41*, 4355; c) F. Delpech, S. Sabo-Etienne, J.-C. Daran, B. Chaudret, K. Hussein, C. J. Marsden, J.-C. Barthelat, *J. Am. Chem. Soc.* **1999**, *121*, 6668; d) I. Atheaux, B. Donnadiou, V. Rodriguez, S. Sabo-Etienne, B. Chaudret, K. Hussein, J.-C. Barthe-

- lat, *J. Am. Chem. Soc.* **2000**, *122*, 5664; e) K. Hussein, C. J. Marsden, J.-C. Barthelat, V. Rodriguez, S. Conejero, S. Sabo-Etienne, B. Donnadieu, B. Chaudret, *Chem. Commun.* **1999**, 1315; f) I. Atheaux, F. Delpech, B. Donnadieu, S. Sabo-Etienne, B. Chaudret, K. Hussein, J. C. Barthelat, T. Braun, S. B. Duckett, R. N. Perutz, *Organometallics* **2002**, *21*, 5347; g) R. H. Said, K. Hussein, J.-C. Barthelat, I. Atheaux, S. Sabo-Etienne, M. Grellier, B. Donnadieu, B. Chaudret, *Dalton Trans.* **2003**, 4139; h) C. Beddie, M. B. Hall, *J. Am. Chem. Soc.* **2004**, *126*, 13564; i) K. S. Cook, Incarvito, C. E. Webster, Y. Fan, M. B. Hall, J. F. Hartwig, *Angew. Chem.* **2004**, *116*, 5590; *Angew. Chem. Int. Ed.* **2004**, *43*, 5474; j) M. Biul, P. Espinet, M. A. Esteruelas, F. J. Lahoz, A. Lledós, J. M. Martínez-Ilarduya, F. Maseras, J. Modrego, E. Oñate, L. A. Oro, E. Sola, C. Valero, *Inorg. Chem.* **1996**, *35*, 1250; k) F. Maseras, A. Lledós, *Organometallics* **1996**, *15*, 1218; l) I. Corral, O. Mó, M. Yáñez, *New J. Chem.* **2003**, *27*, 1657; m) I. Corral, O. Mó, M. Yáñez, *Int. J. Mass Spectrom.* **2003**, *227*, 401; n) I. Corral, O. Mó, M. Yáñez, *Theor. Chem. Acc.* **2004**, *112*, 298; o) I. Corral, O. Mó, M. Yáñez, *J. Phys. Chem. A* **2003**, *107*, 1370; p) M. F. Fan, Z. Lin, *Organometallics* **1999**, *18*, 286; q) S. M. Ng, C. P. Lau, M.-F. Fan, Z. Lin, *Organometallics* **1999**, *18*, 2484; r) S.-H. Choi, Z. Lin, *J. Organomet. Chem.* **2000**, *608*, 42; s) S.-H. Choi, J. Feng, Z. Lin, *Organometallics* **2000**, *19*, 2051; t) D. Liu, K. C. Lam, Z. Lin, *Organometallics* **2003**, *22*, 2827; u) M.-F. Fan, G. Jia, Z. Lin, *J. Am. Chem. Soc.* **1996**, *118*, 9915; v) R. F. W. Bader, C. F. Matta, F. Cortés-Guzmán, *Organometallics* **2004**, *23*, 6253; w) A. Bihlmeier, T. M. Greene, H.-J. Himmel, *Organometallics* **2004**, *23*, 2350; x) H.-J. Himmel, *Chem. Eur. J.* **1997**, *3*, 1608; y) H. Rabaa, J.-Y. Saillard, U. Schubert, *J. Organomet. Chem.* **1987**, *330*, 397.
- [5] Recent review: Z. Lin, *Chem. Soc. Rev.* **2002**, *31*, 239.
- [6] a) G. J. Kubas, R. R. Ryan, B. I. Swanson, P. J. Vergamini, H. Wasserman, *J. Am. Chem. Soc.* **1984**, *106*, 451; b) G. J. Kubas, "Metal Di-hydrogen and σ -Bond Complexes" Kluwer Academic/Plenum, New York **2001**.
- [7] R. H. Crabtree, *Angew. Chem.* **1993**, *105*, 828; *Angew. Chem. Int. Ed. Engl.* **1993**, *32*, 789.
- [8] G. I. Nikonov, *Adv. Organomet. Chem.* **2005**, *53*, 217–309.
- [9] a) K. Hübler, U. Hübler, W. R. Roper, P. Schwerdtfeger, L. J. Write, *Chem. Eur. J.* **1997**, *3*, 1608; b) N. M. Yardy, F. R. Lemke, L. B. Brammer, *Organometallics* **2001**, *20*, 5670; c) S. Lachaize, S. Sabo-Etienne, B. Donnadieu, B. Chaudret, *Chem. Commun.* **2003**, 214; d) F. Delpech, S. Sabo-Etienne, B. Donnadieu, B. Chaudret, *J. Am. Chem. Soc.* **1997**, *119*, 3167; e) F. Delpech, S. Sabo-Etienne, J. C. Daran, B. Chaudret, K. Hussein, C. Marsden, J. C. Barthelat, *J. Am. Chem. Soc.* **1999**, *121*, 6668; f) R. B. Said, K. Hussein, J. C. Barthelat, I. Atheaux, S. Sabo-Etienne, M. Grellier, B. Donnadieu, B. Chaudret, *Dalton Trans.* **2003**, 4139; g) T. Ayed, J. C. Barthelat, B. Tangour, C. Pradere, B. Donnadieu, M. Grellier, S. Sabo-Etienne, *Organometallics* **2005**, *24*, 3824; h) S. Lachaize, S. Sabo-Etienne, *Eur. J. Inorg. Chem.* **2006**, 2115.
- [10] U. Schubert, *Adv. Organomet. Chem.* **1990**, *30*, 151.
- [11] Gaussian 03, Revision C.02, M. J. Frisch, G. W. Trucks, H. B. Schlegel, G. E. Scuseria, M. A. Robb, J. R. Cheeseman, J. A. Montgomery, Jr., T. Vreven, K. N. Kudin, J. C. Burant, J. M. Millam, S. S. Iyengar, J. Tomasi, V. Barone, B. Mennucci, M. Cossi, G. Scalmani, N. Rega, G. A. Petersson, H. Nakatsuji, M. Hada, M. Ehara, K. Toyota, R. Fukuda, J. Hasegawa, M. Ishida, T. Nakajima, Y. Honda, O. Kitao, H. Nakai, M. Klene, X. Li, J. E. Knox, H. P. Hratchian, J. B. Cross, V. Bakken, C. Adamo, J. Jaramillo, R. Gomperts, R. E. Stratmann, O. Yazyev, A. J. Austin, R. Cammi, C. Pomelli, J. W. Ochterski, P. Y. Ayala, K. Morokuma, G. A. Voth, P. Salvador, J. J. Dannenberg, V. G. Zakrzewski, S. Dapprich, A. D. Daniels, M. C. Strain, O. Farkas, D. K. Malick, A. D. Rabuck, K. Raghavachari, J. B. Foresman, J. V. Ortiz, Q. Cui, A. G. Baboul, S. Clifford, J. Cioslowski, B. B. Stefanov, G. Liu, A. Liashenko, P. Piskorz, I. Komaromi, R. L. Martin, D. J. Fox, T. Keith, M. A. Al-Laham, C. Y. Peng, A. Nanayakkara, M. Challacombe, P. M. W. Gill, B. Johnson, W. Chen, M. W. Wong, C. Gonzalez, J. A. Pople, Gaussian, Inc., Wallingford CT, **2004**.
- [12] J. P. Perdew, K. Burke, M. Ernzerhof, *Phys. Rev. Lett.* **1996**, *77*, 3865.
- [13] a) A. Schäfer, C. Huber, R. Ahlrichs, *J. Chem. Phys.* **1994**, *100*, 5829; b) ftp://ftp.chemie.uni-karlsruhe.de/pub/basen/fe.
- [14] I. Mayer, *Chem. Phys. Lett.* **1983**, *97*, 270; corrigendum: I. Mayer, *Chem. Phys. Lett.* **1985**, *117*, 396.
- [15] K. B. Wiberg, *Tetrahedron* **1968**, *24*, 1024.
- [16] a) M. Giambiagi, M. S. Giambiagi, K. C. Mundim, *Struct. Chem.* **1990**, *1*, 423; b) T. Kar, A. B. Sannigrahi, *Chem. Phys. Lett.* **1990**, *173*, 569; c) R. Ponec, I. Mayer, *J. Phys. Chem. A* **1997**, *101*, 1738.
- [17] R. Ditchfield, *J. Chem. Phys.* **1976**, *65*, 3123.
- [18] W. Kutzelnigg, U. Fleischer, M. Schindler in *NMR Basic Principles and Progress, Vol. 23* (Eds.: P. Diehl, E. Fluck, H. Günther, R. Kosfeld, J. Seelig), Springer, Berlin, **1990**, p. 165.
- [19] T. Helgaker, M. Watson, N. C. Handy, *J. Chem. Phys.* **2000**, *113*, 9402.
- [20] a) A. D. Becke, *Phys. Rev. A* **1988**, *38*, 3098; b) C. Lee, W. Yang, R. G. Parr, *Phys. Rev. B* **1988**, *37*, 785; c) B. Miehlich, A. Savin, H. Stoll, H. Preuss, *Chem. Phys. Lett.* **1989**, *157*, 200; d) A. D. Becke, *J. Chem. Phys.* **1993**, *98*, 5648.
- [21] a) A. D. Becke, *J. Chem. Phys.* **1997**, *107*, 8554; b) A. D. Becke, *Inorg. Chem.* **1970**, *9*.
- [22] W. Jetz, W. A. G. Graham, *Inorg. Chem.* **1971**, *10*, 1159.
- [23] a) C. Gordon, U. Schubert, *Inorg. Chim. Acta* **1994**, *224*, 177; b) unpublished work of W. Malisch and H. Käß cited as reference [5] in reference [23a].
- [24] L. Manojlović-Muir, K. W. Muir, J. A. Ibers, *Inorg. Chem.* **1970**, *9*, 447.
- [25] R. A. Smith, M. J. Bennett, *Acta Crystallogr. Sect. B* **1977**, *33*, 1118.
- [26] K. A. Simpson, Ph.D. Thesis, University of Alberta, **1973**.
- [27] a) P. Kubáček, R. Hoffmann, Z. Havlas, *Organometallics* **1982**, *1*, 180, and references therein. b) R. Poli, *Organometallics* **1990**, *9*, 1892, and references therein; c) Z. Lin, M. B. Hall, *Organometallics* **1992**, *11*, 3801; d) Z. Lin, M. B. Hall, *Organometallics* **1993**, *12*, 19.
- [28] P. Hofmann, M. Padmanabhan, *Organometallics* **1983**, *2*, 1273.
- [29] a) T. A. Albright, *Tetrahedron* **1982**, *38*, 1339; b) R. Hoffmann, *Science* **1981**, *211*, 995; c) T. A. Albright, J. K. Burdett, M.-H. Whangbo, *Orbital Interactions in Chemistry*, Wiley, New York, **1985**.
- [30] a) S. K. Ignatov, N. H. Rees, B. R. Tyrrell, S. R. Dubberley, A. G. Razuvaev, P. Mountford, G. I. Nikonov, *Chem. Eur. J.* **2004**, *10*, 4991; b) K. Yu. Dorogov, E. Dumont, N.-N. Ho, A. V. Churakov, L. G. Kuzmina, J.-M. Poblet, A. J. Schultz, J. A. K. Howard, R. Bau, A. Lledós, G. I. Nikonov, *Organometallics* **2004**, *23*, 2845; c) S. R. Dubberley, S. K. Ignatov, N. H. Rees, A. G. Razuvaev, P. Mountford, G. I. Nikonov, *J. Am. Chem. Soc.* **2003**, *125*, 644; d) G. I. Nikonov, L. G. Kuzmina, J. A. K. Howard, *J. Chem. Soc. Dalton Trans.* **2002**, 3037; e) G. I. Nikonov, P. Mountford, S. K. Ignatov, J. C. Green, P. A. Cooke, M. A. Leech, L. G. Kuzmina, A. G. Razuvaev, N. H. Rees, A. J. Blake, J. A. K. Howard, D. A. Lemenovskii, *Dalton Trans.* **2001**, 2903; f) V. I. Bakhturov, J. A. K. Howard, D. A. Keen, L. G. Kuzmina, M. A. Leech, G. I. Nikonov, E. V. Vorontsov, C. C. Wilson, *J. Chem. Soc. Dalton Trans.* **2000**, 1631; g) G. I. Nikonov, L. G. Kuzmina, S. F. Vyboishchikov, D. A. Lemenovskii, J. A. K. Howard, *Chem. Eur. J.* **1999**, *5*, 2497.
- [31] H. A. Bent, *Chem. Rev.* **1961**, *61*, 275.
- [32] J. Y. Corey, J. Braddock-Wilking, *Chem. Rev.* **1999**, *99*, 175.
- [33] M. F. Fan, Z. Lin, *Organometallics* **1998**, *17*, 1092.
- [34] M. Bühl, F. T. Mauschick, *Organometallics* **2003**, *22*, 1422.
- [35] a) R. F. W. Bader, *Atoms in Molecules: A Quantum Theory*, Clarendon, New York, **1990**; b) R. F. W. Bader, H. Essén, *J. Chem. Phys.* **1984**, *80*, 1943; c) R. F. W. Bader, P. J. MacDougall, *J. Am. Chem. Soc.* **1985**, *107*, 6788.
- [36] a) D. Cremer, E. Kraka, *Angew. Chem.* **1984**, *96*, 612; b) D. Cremer, E. Kraka, *Croat. Chem. Acta* **1984**, *57*, 1259.
- [37] a) A. L. Osipov, S. F. Vyboishchikov, K. Y. Dorogov, L. G. Kuzmina, J. A. K. Howard, D. A. Lemenovskii, G. I. Nikonov, *Chem. Commun.* **2005**, 3349; b) G. I. Nikonov, S. F. Vyboishchikov, L. G. Kuzmina, J. A. K. Howard, *Chem. Comm.* **2002**, 568.
- [38] Some examples of theoretical work on *cis* effect: a) S. A. Jackson, O. Eisenstein, *Inorg. Chem.* **1990**, *29*, 3910; b) F. Maseras, M. Duran, A. Lledós, J. Bertrán, *J. Am. Chem. Soc.* **1992**, *114*, 2922; c) F. Mase-

- ras, M. Duran, A. Lledós, J. Bertrán, *J. Am. Chem. Soc.* **1991**, *113*, 2879; d) J.-F. Riehl, M. Péliissier, O. Eisenstein, *Inorg. Chem.* **1992**, *31*, 3344; e) L. S. van der Sluys, J. Eckert, O. Eisenstein, J. H. Hall, J. C. Huffman, S. A. Jackson, T. F. Koetzle, G. J. Kubas, P. J. Vergamini, K. G. Caulton, *J. Am. Chem. Soc.* **1990**, *112*, 4831; f) C. Bianchini, D. Masi, M. Peruzzini, M. Casarin, C. Maccato, G. A. Rissi, *Inorg. Chem.* **1997**, *36*, 1061; g) related work: H. Jacobsen, H. Berke, *Chem. Eur. J.* **1997**, *3*, 881.
- [39] a) D. M. Heinekey, A. Lledós, J. M. Lluch, *Chem. Soc. Rev.* **2004**, *33*, 175; b) R. Gelabert, M. Moreno, J. M. Lluch, A. Lledós, D. M. Heinekey, *J. Am. Chem. Soc.* **2005**, *127*, 5632; c) R. Gelabert, M. Moreno, J. M. Lluch, *Chem. Eur. J.* **2005**, *11*, 6315; d) D. G. Gusev, *J. Am. Chem. Soc.* **2004**, *126*, 1424; e) R. Gelabert, M. Moreno, J. M. Lluch, A. Lledós, *J. Am. Chem. Soc.* **1997**, *119*, 9840; f) R. Gelabert, M. Moreno, J. M. Lluch, A. Lledós, V. Pons, D. M. Heinekey, *J. Am. Chem. Soc.* **2004**, *126*, 8813.
- [40] For leading references on the calculation of NMR chemical shifts and coupling constants, see: a) "The Calculation of NMR Parameters in Transition Metal Complexes": J. Autschbach in *Principles and Applications of Density Functional Theory in Inorganic Chemistry*, Vol. 112 (Eds.: N. Kaltsoyannis, J. E. McGrady), Springer, Heidelberg, **2004**; b) "Relativistic Calculation of Spin-Spin Coupling Constants": J. Autschbach, T. Ziegler in *Calculation of NMR and EPR Parameters. Theory and Applications* (Eds.: M. Kaupp, M. Bühl, V. G. Malkin), Wiley-VCH, Weinheim, **2004**; c) "Relativistic Computation of NMR Shieldings and Spin-spin Coupling Constants": J. Autschbach, T. Ziegler in *Encyclopedia of Nuclear Magnetic Resonance* Vol. 9 (Eds.: D. M. Grant, R. K. Harris), Wiley, Chichester, **2002**; d) for the calculation of NMR parameters in dihydrogen complexes, see references [40c–e] and B. Le Guennic, S. Patchkovskii, J. Autschbach, *J. Chem. Theory Comput.* **2005**, *1*, 601, and references therein.
- [41] a) K. K. Pandey, M. Lein, G. Frenking, *Organometallics* **2004**, *23*, 2944; b) R. West, J. J. Buffy, M. Haaf, T. Müller, B. Gehrus, M. F. Lappert, Y. Apeloig, *J. Am. Chem. Soc.* **1998**, *120*, 1639.
- [42] For the recent calculation of the ^{29}Si chemical shifts in disylenes see: a) M. Karni, Y. Apeloig, N. Takagi, S. Nagase, *Organometallics* **2005**, *24*, 6319; b) D. Auer, M. Kaupp, C. Strohmann, *Organometallics* **2005**, *24*, 6331.
- [43] Calculations of Si–H coupling constants became available only recently: a) D. L. Lichtenberger, *Organometallics* **2003**, *22*, 1599; b) reference [37a].
- [44] P. Atkins, J. de Paula, *Atkins' Physical Chemistry*, 7th edition, Oxford, **2002**, p. 632.
- [45] G. I. Nikonov, *Organometallics* **2003**, *22*, 1597.
- [46] Although there several literature precedents of polyhydride silyl and polysilyl hydride complexes containing η^2 -silane unit, there are either fluxional or exhibit distinctive "secondary" interligand interactions. In the latter case, the description in terms of hypervalent silyl ligands $(\text{H}_3\text{SiR}_3)^{2-}$ and $(\text{H}_2\text{SiR}_3)^-$ is a viable alternative.^[8]

Received: March 28, 2006
Published online: August 10, 2006